# FINITE ELEMENT ANALYSIS OF CERVICAL SPINE & FINITE ELEMENT MODELING OF KNEE JOINT

A THESIS SUBMITTED TO

THE GRADUATE SCHOOL OF

ENGINEERING AND NATURAL SCIENCES

OF ISTANBUL MEDIPOL UNIVERSITY

IN PARTIAL FULFILLMENT OF THE REQUIREMENTS FOR

THE DEGREE OF

MASTER OF SCIENCE

IN

BIOMEDICAL ENGINEERING AND BIOINFORMATICS

By

Muzammil Mumtaz

August, 2017

# ABSTRACT

## FINITE ELEMENT ANALYSIS OF CERVICAL SPINE & FINITE ELEMENT MODELING OF KNEE JOINT

Muzammil Mumtaz
M.S. in Biomedical Engineering and Bioinformatics
Advisor: Assist. Prof. Dr. Deniz Ufuk Erbulut
August, 2017

Finite Element (FE) analysis allows predicting the behavior of real life systems in controlled environment. In the recent decades, FE modeling has gained significant attention of the medical industry as well. There is no chance of error in the surgical operations. Therefore, medical professionals seek for a solution that would predict the behavior of implants inside the human body so the surgeon can opt for a best possible treatment.

This thesis is based on FE modeling. This thesis can be divided into two major studies i.e. 1) FE analysis of cervical spine with implants and 2) development and validation of knee joint.

For developing FE knee model, computerized tomographic (CT) scans were used to acquire accurate geometry of knee joint. The CT scans were used to construct a 3D model of knee joint in Mimics software. The geometry of all the soft tissues was obtained from literature. For the application of muscle's force, connector elements were used.

The FE model of upper cervical (C0-C2) was used to study the biomechanical effect of three popular screw based atlantoaxial fixation constructs on the cervical spine. On the other hand, FE model of cervical (C2-C7) was used to study the effect of multi-level disc replacement and fusion on cervical spine. The dynamic cervical implant (DCI) was used for the disc replacement purpose.

This thesis introduces a novel method for the development of soft tissues of the knee joint which makes the knee model more realistic. Besides this, effects caused by implants on spine biomechanics reported in this thesis are of clinical significance for surgeons.

*Keywords:* Finite element, knee biomechanics, cervical spine, atlantoaxial fixation.

# ÖZET

# SERVİKAL OMURUN SONLU ELEMAN ANALİZİ & DİZ EKLEMİNİN SONLU ELEMAN MODELLEMESİ

Muzammil Mumtaz
Biyomedikal Mühendisliği ve Biyoenformatik, Yüksek Lisans
Tez Danışmanı: Yrd. Doç. Dr. Deniz Ufuk Erbulut
Ağustos, 2017

Sonlu Elemanlar (FE) analizi, kontrollü ortamdaki gerçek yaşam sistemlerinin davranışı tahminini sağlar. Son yıllardaki FE modellemeleri tıp endüstrisinde önem arz etmektedir. Cerrahi ameliyatlardaki hata olasılığı yok denecek düzeyde düşük olması gerekmektedir. Bu nedenle, tıp uzmanları, cerrahlar için mümkün olan en iyi tedaviyi seçebilmesi için insan vücudundaki implantların davranışını öngörecek bir çözüm arayışındadır.

Bu tez, FE modellemesi içeren iki çalışmadan oluşmaktadır. Bu çalışmalar; Implantlarla servikal omurganın FE analizi ve 2) diz ekleminin gelişimi ve geçerliliği. FE diz modelinin geliştirilmesi için diz ekleminin doğru geometrisini elde edilmesi gerekmektedir. Bunun için bilgisayarlı tomografik (BT) taramalar kullanılmıştır. BT taramaları, Mimics yazılımında bir diz eklemi 3 boyutlu modeli oluşturmak için kullanılmıştır. Tüm yumuşak dokuların geometrisi ise literatürden elde edilmiştir. Kas kuvvetinin uygulanması için bağlantı elemanları kullanılmıştır.

Servikal omurgadaki atlantoaksiyel fiksasyon yapılarının üç yapılı vidaya dayalı biyomekanik etkisini incelemek için üst servikal FE modeli (C0-C2) kullanılmıştır. Öte yandan, çok seviyeli disk replasmanı ve servikal omurga üzerine füzyonun çalışması için servikal (C2-C7) FE modeli kullanılmıştır. Disk değiştirme amacı için dinamik servikal implant (DCI) kullanılmıştır.

Bu çalışma diz ekleminin yumuşak dokularının geliştirilmesi için diz modelini daha gerçekçi hale getiren yeni bir yöntem ortaya koymaktadır. Bunun yanında, belirtilen omurga biyomekaniğinde implantların neden olduğu özellikler cerrahlar için klinik önem arz etmektedir.

*Anahtar sözcükler*: Sonlu elemanlar, diz beyomekaniği, servikal omurga, atlantoaksial fiksasyon.

# Acknowledgement

First of all I would like to acknowledge my supervisor Dr. Deniz Ufuk Erbulut for his guidance and support throughout my master's program. His knowledge and great research experience helped me in completing my degree.
Secondly, I would like to acknowledge senior member of our group Dr. Iman Zafarparandeh for his continuous guidance and support with technical challenges that I faced during my education.
Moreover, I would like to thank my parents and family for their moral support and for always supporting me to pursue higher education.
I would like to thank my lab members and all my colleagues in the university.
I would also like to thank Istanbul Medipol University for providing me with the necessary tools and logistics to accomplish my tasks.

# Contents

# List of Figures

# List of Tables

# Chapter 1

# Introduction

Finite Element (FE) modeling is a tool which is used to simulate the real world scenarios in different aspects of engineering. With the advancements in computing technology, it is now possible to develop accurate FE-Models. There were 2 main objectives of this thesis; 1) developing FE knee model, 2) FE analysis of cervical spine and its instrumentation.

The knee joint model was developed from the scratch including the geometry of bones and soft tissues and validated it against other in vitro and FE studies. In the previous FE-Models of the knee joint, the geometry of soft tissues was not taken into account as their geometry is not easy to obtain from computerized tomography (CT) and magnetic resonance imaging (MRI) scans so they were replaced by using simple truss elements. However, in the recent models, researchers have developed the models including soft tissues but there is a need of more models in the literature to have a more accurate model. For the development of knee model, the first step was to acquire accurate geometry. The accuracy of the geometry was verified with literature as well as with medical doctors. To obtain the geometry of bones CT scans were used and ligaments morphology was obtained from literature.

For the cervical spine biomechanical analysis, previously validated model of

intact spine was used. The cervical spine can be theoretically divided into two main regions i.e. C0-C2 and C2-C7. The C0-C2 atlantoaxial region with skull was studied by incorporating three constructsa transarticular screw (C1-C2TA), a lateral mass screw in C1 and pedicle screw in C2 (C1LM-C2PD), and a lateral mass screw in C1 and translaminar screw in C2 (C1LM-C2TL). Moreover, for predicting the behaviour of these constructs in injured spine, type II dens fracture was induced in the intact model to produce an injured model. From C2-C7 the cervical spine was used for simulating 1) single level disc replacement, 2) bi-level disc replacement, 3) hybrid surgery that incorporates implantation adjacent to fusion, 4) single level fusion, 5) bi-level fusion. For the cases involving disc replacement, dynamic cervical implant (DCI) was used which is a standalone U-shaped implant and has not been studied in much detail in literature.

All the models were simulated in ABAQUS and the output from ABAQUS was processed in MATLAB by writing custom scripts. Besides this MIMICS software was used to construct 3D geometry of bones from CT scans. IA-FE Mesh was used to mesh all the 3D geometries and Solidworks software was used to develop ligaments for knee joint as well as for developing implants for cervical spine.

The goal of this thesis was to use FE model of cervical spine to study the biomechanical effect of spinal devices on the cervical spine and develop a FE model of knee joint. Chapter 2 contains the details of anatomy and physiology of cervical spine and knee joint. Chapter 3 provides a literature review on cervical spine instrumentation biomechanics and knee joint biomechanics. Chapter 4 contains the study and FE model of atlantoaxial region used to study three atlantoaxial screw based fixation techniques. Chapter 5 contains the study and FE model of cervical (C2-C7) used for multi-level disc replacement and multi-level fusion. Chapter 6 provides a detailed method for developing the finite element of knee joint.

# Chapter 2

# Anatomy and Physiology

## 2.1 Anatomy and physiology of cervical spine

The cervical spine (neck) has seven segments and is more mobile as compared to thoracic and lumbar spine. For better understanding of cervical spine biomechanics, we can divide cervical spine into two regions i.e. upper cervical (C0-C2) and the rest (C2-C7).

### 2.1.1 C0-C2

The upper cervical (Atlantoaxial region) is composed of complex bony vertebrae i.e. atlas and axis along with ligaments. This combination of bones and ligaments allow a wide variety of complex motion at this junction [1–5]. The atlas is attached to the occiput and the physiological structure of atlas allows flexion and extension between occiput and atlas. Besides flexion and extension atlas and occiput move as a single unit during lateral bending and axial rotation [6]. However, in cadaver studies we observe lateral bending and axial rotation being artificially produced by fixing C1 or C2 and forcing the head to move in all directions. Furthermore, atlas sits on the axis and the weight of the skull is transferred from atlas to axis

and to the following spine. There is no intervertebral disc in atlantoaxial region and this junction is solely stabilized by ligaments and facets. In order to provide axial rotation to the head, atlas sits on the odontoid process of axis which serves as a pivot point for rotation. The axial rotation is achieved when the anterior arch of the atlas slides around the dens. The rotational stability of upper cervical spine is provided by alar ligament whereas transverse ligament prevents excessive flexion and anterior displacement of C1 vertebrae [7]. Further stability during flexion and extension is provided by atlantoaxial anterior and posterior ligament respectively. The rotation in this junction is higher as compared to any other region in spine.

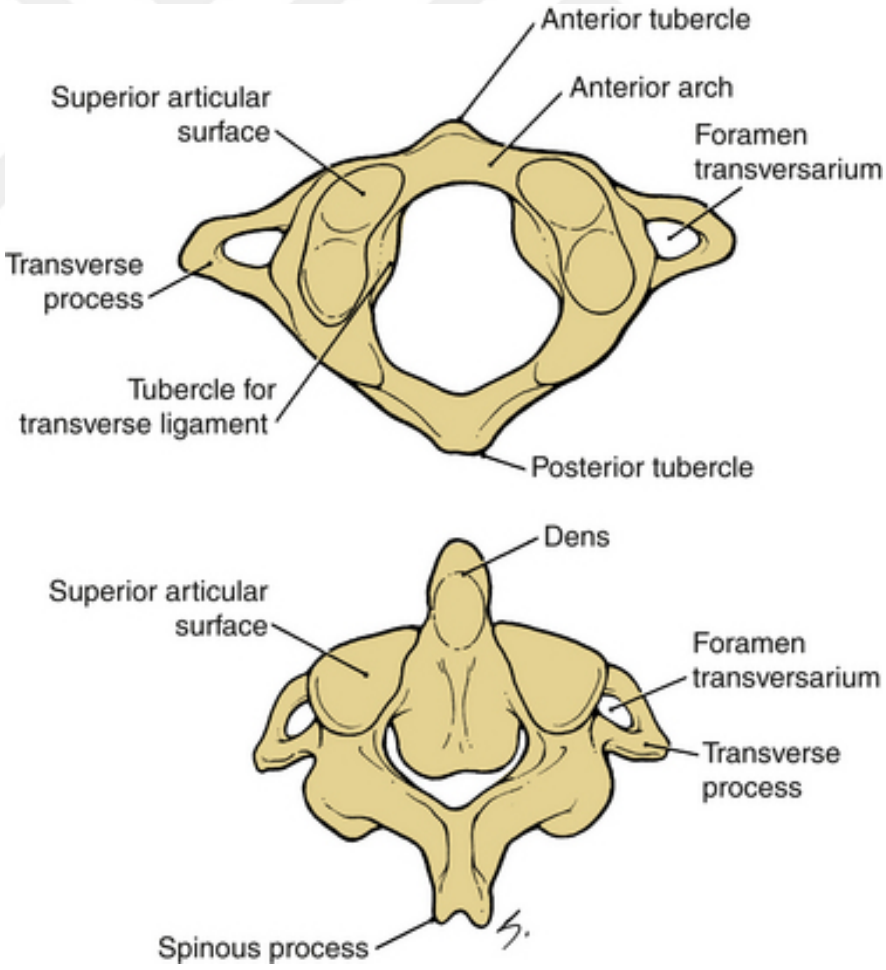


Figure 2.1: Bony anatomy of C0-C2 region [8]

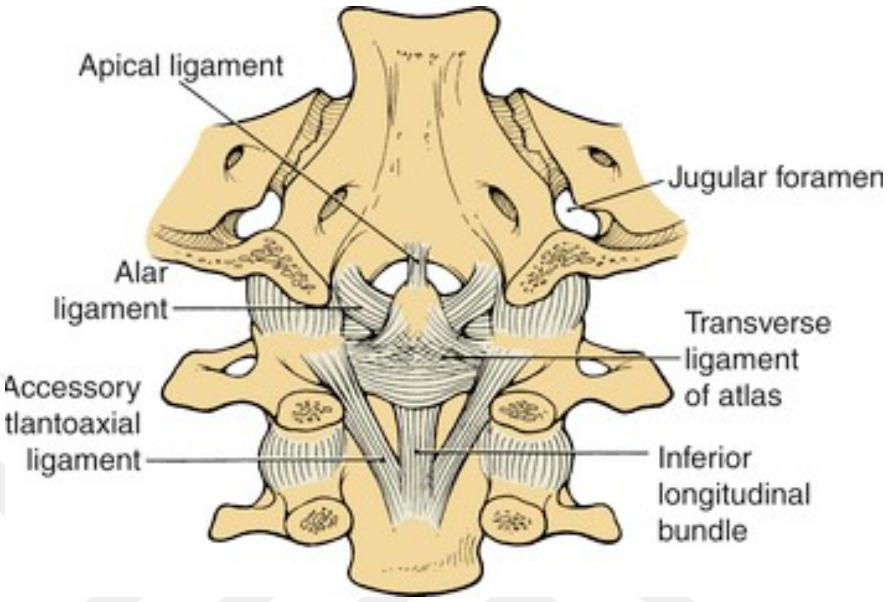


Figure 2.2: Ligaments anatomy of C0-C2 region [8]

### 2.1.2 C2-C7

The vertebrae of cervical spine have an anterior-posterior curvature as well as medial-lateral curvature. These vertebral bodies are stacked on top of each other and form the lordotic curvature [9, 10]. The lorodotic curvature of cervical spine is measured by the four-line Cobb method. The C1 is the smallest vertebrae and the size of following vertebrae gets bigger and bigger as they need to support more weight. The cervical spine has an intervertebral disk between the vertebras C2-C7. The intervertebral disc has a thick outer layer consisting of crisscrossing fibrous structure that surrounds the nucleus which is a soft structure such as gel. The intervertebral disc plays an important role in distributing the load uniformly from upper vertebra to the following lower vertebra. Moreover, intervertebral disc serves as shock absorber for the neck and facilitates the motion of neck such as bending sideways or nodding the head. The motion of cervical spine is also guided and limited by the facet joints present at the back of vertebra on the lateral sides. The sides of each facet joint are covered by articular cartilage which reduces the friction between the joint and allows smooth motion. The motion of cervical spine directly affects the openings of nerve root i.e. neural foramina which are present between each vertebral segment. The nerve roots

exiting from neural foramina connect to different part of the body carrying the stimulus from the brain. The opening of neural foramina gets larger during flexion and gets smaller during extension. Similarly, during right lateral bending the left neural foramina opening will get larger and vice versa. Besides neural foramina, all the vertebras form a cavity behind the intervertebral disc known as spinal canal or neural canal. The spinal cord passes through this canal and the vertebral bodies serve as a protection cage for it. The size of spinal canal increases during flexion and decreases during extension. Since, the motion happening in the neck is complex, it is facilitated by the soft tissues as well. The flexion of the cervical spine is facilitated by ligamentum nuchae, ligamentum flavum, posterior longitudinal ligament and interspinous ligaments. Whereas, extension movement of cervical spine is restricted by anterior longitudinal ligament. Furthermore, capsular ligaments provide stability to the facet joints [11].

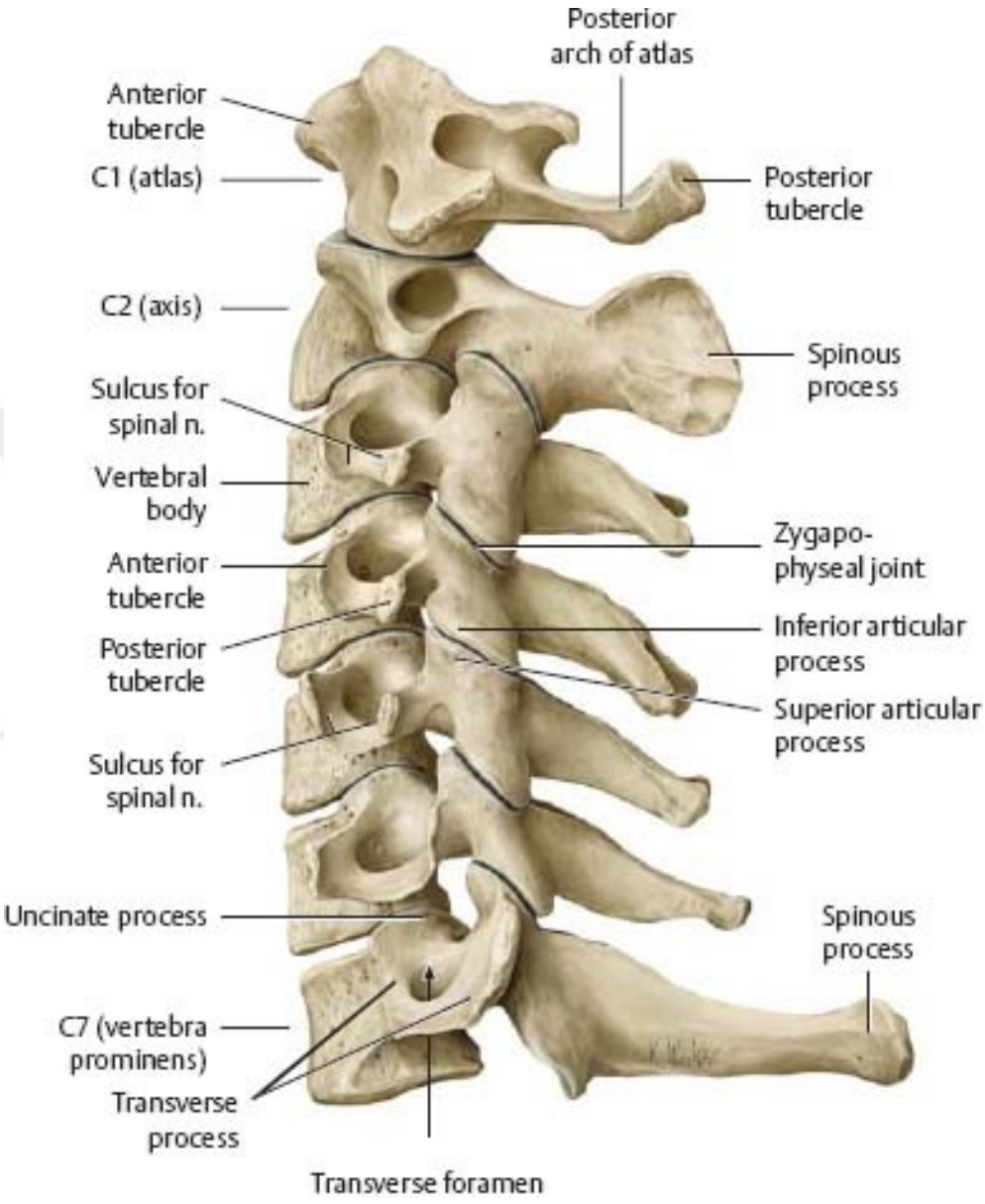


Figure 2.3: Bony anatomy of cervical spine [12]

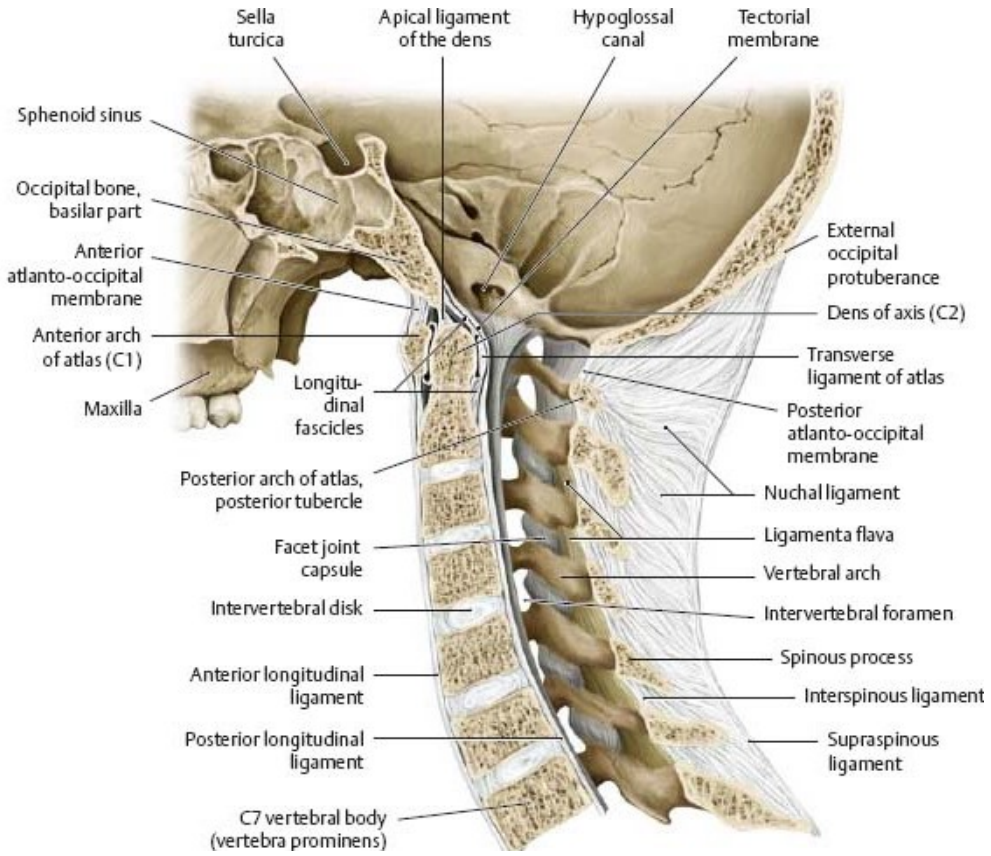


Figure 2.4: Ligaments anatomy of cervical spine [12]

## 2.2 Knee Joint

Knee joint is the largest and most complex joint in the human skeleton, it is composed of four bones i.e. femur, tibia, patella and fibula. This joint consists of soft tissues which contribute significantly to the joint motion such as meniscus, anterior cruciate ligament (ACL), posterior cruciate ligament (PCL), lateral collateral ligament (LCL) and medial collateral ligament (MCL). The extreme end contact surface of the bones is covered with cartilages to reduce the friction between the bones and the joint is further lubricated by the synovial fluid to reduce the friction between cartilages.

### 2.2.1 Femur

The femur (thigh) bone is regarded as the longest and strongest bone in the human skeleton and can resist impact of upto 2500pounds [13]. Theoretically femur can be divided into three sections i.e. proximal, shaft and distal. The proximal femur contains the head of the femur which has a cylindirical shape and that fits into the pelvis to form a hip joint which acts as a ball and socket joint. As the shaft of the femur runs down from hip to the knee joint it inclines medially in order to provide stability by getting the knee joint close to center of gravity of the body [14]. The distal end of the femur contains medial and lateral condyle that sits on the tibia. The distal femur serves as an attachment region for ligaments such as ACL, PCL, LCL, MCL, medial patellofemoral ligament (MPFL), lateral patellofemoral ligament (LPFL) etc are attached to the distal femur.

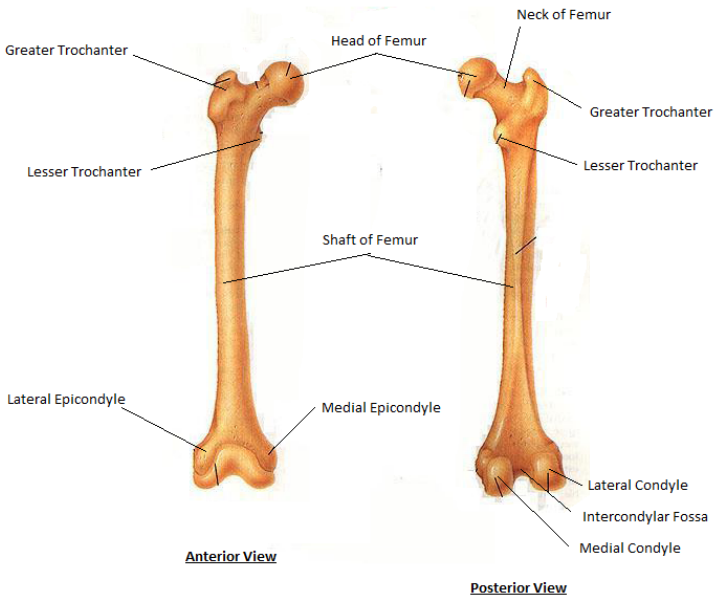


Figure 2.5: Anatomy of femur [14]

### 2.2.2 Tibia

The tibia (shin) bone is regarded as the second longest bone in the human skeleton [15]. The weight of the body is transferred from femur to the tibia and therefore sometimes tibia is termed as weight bearing bone. The proximal tibia i.e. medial and lateral condyles of tibia experience the load from femoral condyles. The tibial shaft transfer the load from proximal tibia to the distal tibia, the surface of tibia increases at the distal end and attaches with ankle. Tibial plateau serves as the attachment region for soft tissues such as ACL and PCL. Moreover, patella tendon is attached to the front of the tibia i.e. tibial tuberosity.

### 2.2.3 Fibula

The fibula bone is located at the lateral side of tibia and runs parallel to it. Fibula is relatively thinner than tibia. The proximal end of the fibula serves as an attachment for LCL which provides stability to the joint and restricts excessive lateral movement of the knee joint. The distal end of the fibula contributes significantly in ankle joint as it forms lateral malleolus which articulates with the tarsal bones [16].

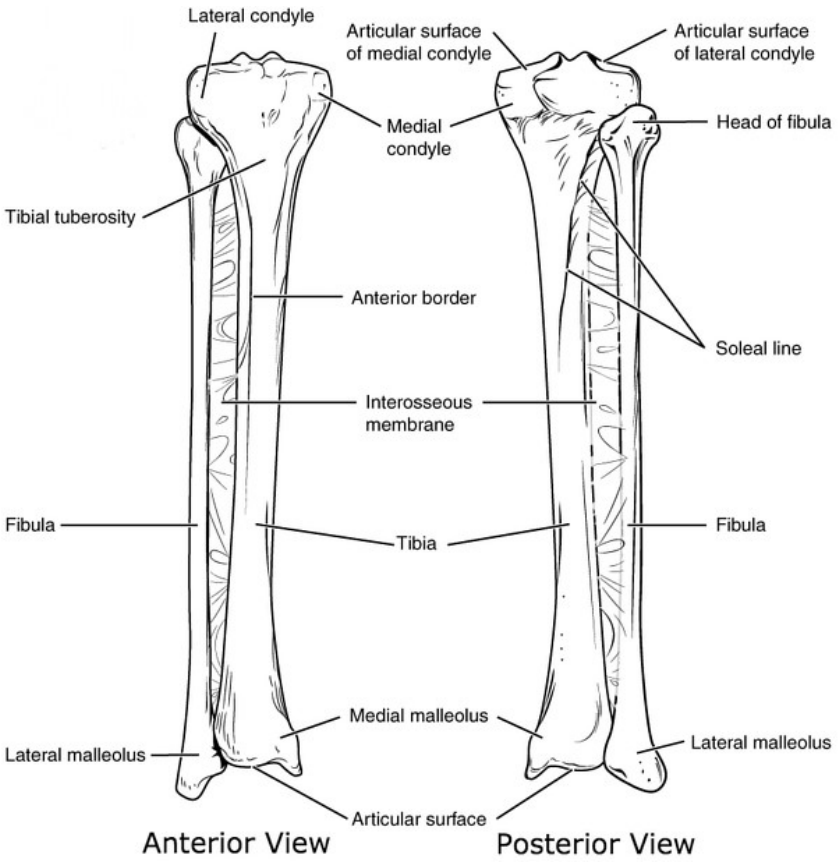


Figure 2.6: Anatomy of tibia and fibula [17]

### 2.2.4 Patella

The patella (knee cap) is present at the front of the knee joint and protects the knee joint against external forces which may lead to injury. The lower end of patella is attached with the patella tendon which is connected to the tibial tuberosity. The upper end of patella is connected with the quadriceps. Morever, patella slides over the femoral grove and facilitates the transfer of muscle force to the femur [18].

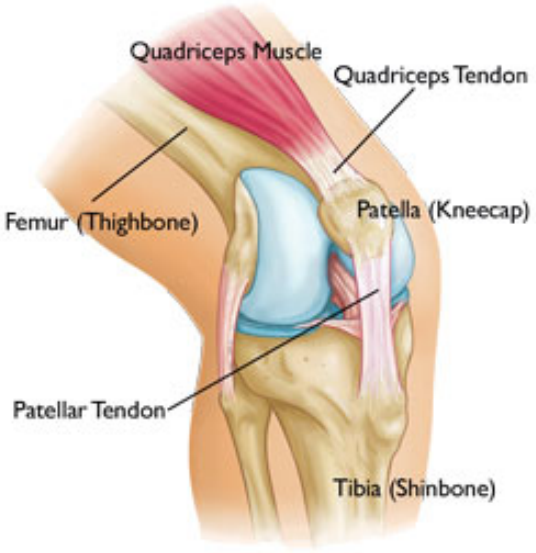


Figure 2.7: Anatomy of patella [19]

### 2.2.5 Meniscus

Knee joint consists of two menisci which have a wedge shaped cross-sectional area [20]. The menisci are located on the medial and lateral side of the knee. The horns and the periphery of the meniscus is attached to the tibia whereas proximal end of meniscus contacts with the femoral condyles. The menisci serve as a schock absorber in the joint and distrbutes the weight evenly to the tibial plateau. Moreover, meniscus contributes to the stability of knee joint during during motion.

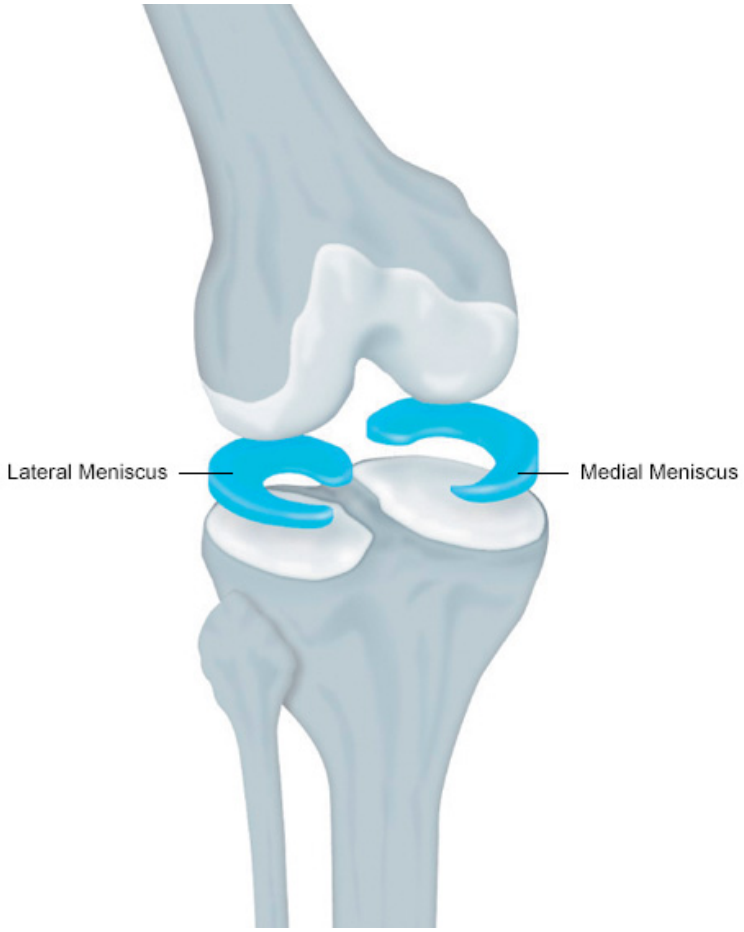


Figure 2.8: Anatomy of meniscus [21]

### 2.2.6 Articular Cartilages

Knee joint consists of four different cartilages; 1)femoral cartilage, 2) tibial cartilage, 3) patellar cartilage and 4) fibular cartilage. The femoral cartilage is the most significant cartilage as it contributes more than other cartilages in the joint movement. The cartilage of femur is present at the distal end of femur and is in contact with meniscus, tibial cartilage and the patellar cartilage. The cartilage of tibia is present on top of the medial and lateral tibial plateaue. Whereas patellar cartilage is present at the posterior/inner side of the patella where it makes contact with femur and slides in femoral grove during movement. Besides this, there is a small fibular cartilage present at the top of fibula where fibula tibiofibular is

formed. The main function of articular cartiladges is to permit smooth motion and load transmission between the bones that form up the joint. The degeneration of articular cartilages can lead to bone diseases such as osteoarthritis.

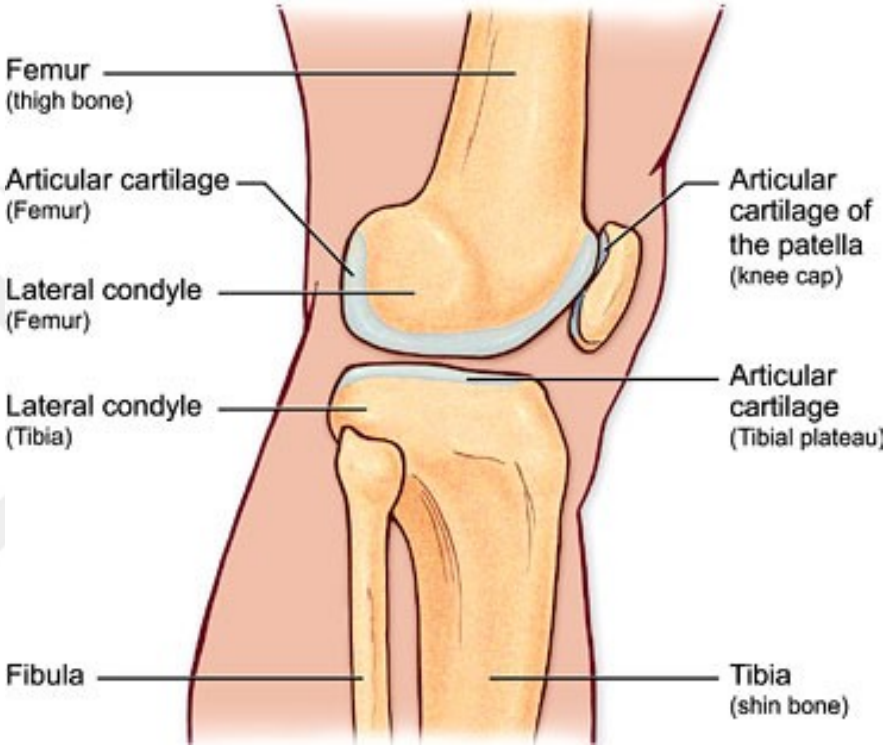


Figure 2.9: Articular Cartilages [22]

### 2.2.7 Ligaments

The function of the knee is complex so it is facilitated by the soft tissues such as ACL, PCL, LCL, MCL, MPFL, LPFL, capsular ligaments and meniscus. The purpose of these soft tissues is to keep the knee intact and prevent it from abnormal motion. However, cruciate and collateral ligaments contribute more than other ligaments. The main function of ACL is to resist the anterior translation of tibia relative to the femur and it also provides resistance to rotational loads. The PCL provides stability to the knee joint by resisting the posterior translation of tibia relative to the femur. Similarly, LCL provides stability to the knee joint against load that tend to move tibia laterally. Besides this MCL provides

stability to the joint against forces that may move tibia medially relative to the femur.

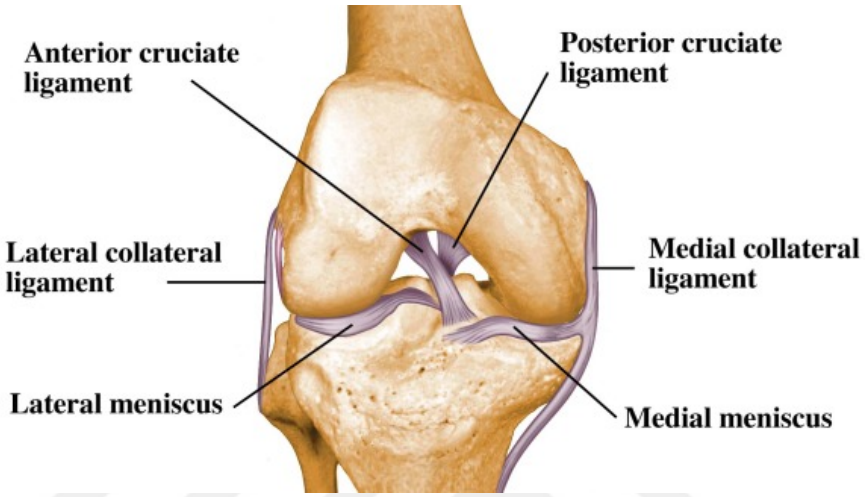


Figure 2.10: Ligaments of the knee joint [23]

### 2.2.8 Muscles and Tendons

The knee joint consists of tendons which are dense elastic tissues and connect the muscles with the bone. The patellar tendon attaches the patella with the tibia. However, quadricep muscles are connected to the top of patella with the quadricep tendon. The quadricep and patellar tendon work in conjunction to straighten the leg [24]. Besides this, hamstring tendon and muscle group is present at the back of the leg. Hamstring muscles run down from pelvis to the lower and help in bending the knee [25].

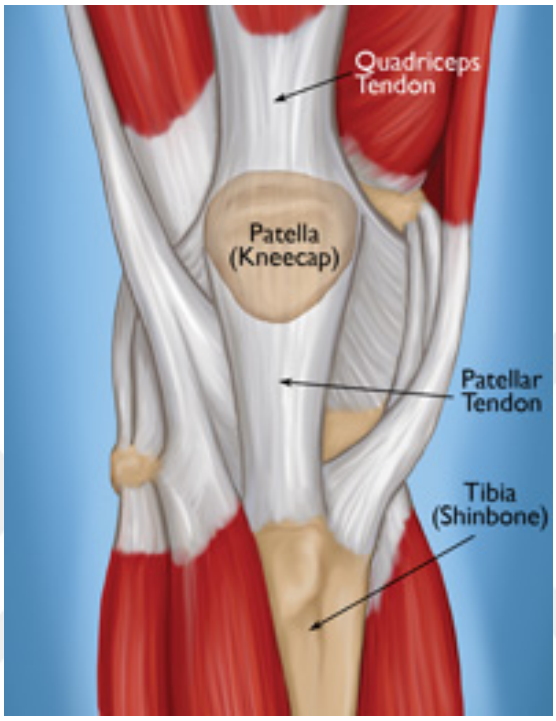


Figure 2.11: Patella and quadriceps tendon [24]

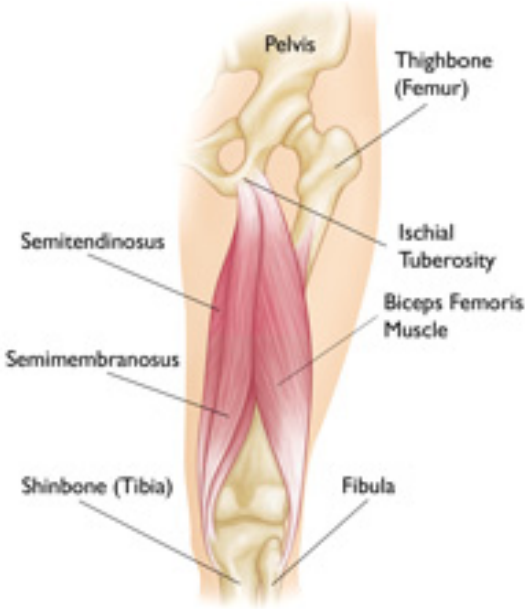


Figure 2.12: Hamstring muscles and tendon [25]

# Chapter 3

# Literature Review

## 3.1 Cervical Spine and Instrumentation Biomechanics

### 3.1.1 Atlantoaxial Instrumentation

Posterior atlantoaxial fixation is an effective method for fusing the antlantoaxial region. The first method for upper cervical fixation was reported in 1939 by Gallie [26], which involved the use of sublaminar wires. Since Gallies wiring technique had low rotational stability. Brooks-Jenkins introduced another wiring technique that provided better rotational stability as compared to Gallies technique while maintaining the similar stability in other directions [27, 28]. However, with the use of sublaminar wires, there is always a chance of spinal cord injury. Therefore, braided cables replaced sublaminar wires to reduce the risk of spinal cord injury [29–31]. The limitations associated with the wiring technique leaded to the development of more reliable methods. Currently, various alternative methods to wiring technique are present.

Over the years, much advancement in posterior atlantoaxial fixation techniques

has been reported. Transarticular and screw-rod fixation techniques are one of the widely accepted treatments for fusion at upper cervical. The Harms method [32] was proposed in 1994 and it is basically the modified version of Goel-Laheris screw-plate system [33]. Despite fusing the vertebrae to great extent this system had a major drawback that the C2 nerve had to be sacrificed during the atlantoaxial fixation [34]. However, Goel-Laheris method was later modified by Harms and Melcher in 2001 which involved the use of C1 lateral mass screw and C2 Pedicle screw along with the rod connecting C1 and C2. Besides Harms technique, Magerl transacrticular screw method [35] is considered as gold standard for posterior atlantoaxial fixation which involves the use of two transarticular screws which are inserted in axis directed towards the anterior arch of the atlas. The Magerl's method has a drawback that it cannot be used in the patients with thoracic kyphosis because of the complexity of placement of screws [35]. Moreover due to close proximity of the vertebral arteries and variable location of the foramen transversarium the placement of transarticular and C2 pedicle screw gets technically complicated [36]. In response to that technical difficulty, Wright 25[21]suggested the use of bilateral, crossing C2 laminar screws along with C1 lateral mass screws similar to Harms.

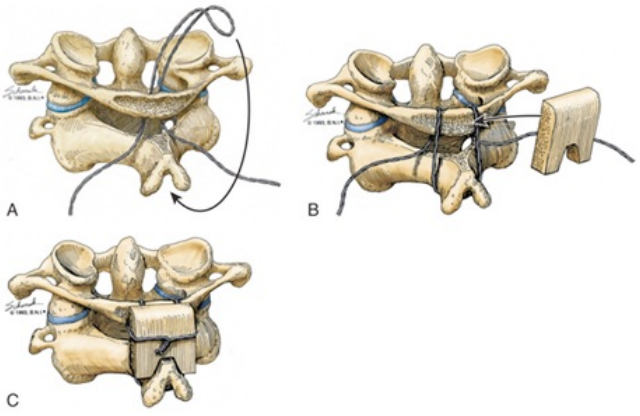


A) A loop wire is passed beneath C1 and fixed beneath the C2 spinous process; B) A notched unicortical bone graft is fitted over the C2 spinous process and positioned behind C1 ring; C) The free ends of the wire are wrapped behing the graft.

Figure 3.1: Gallies Wiring Technique (Copyright 1993, Barrow Neurological Institute) [37]

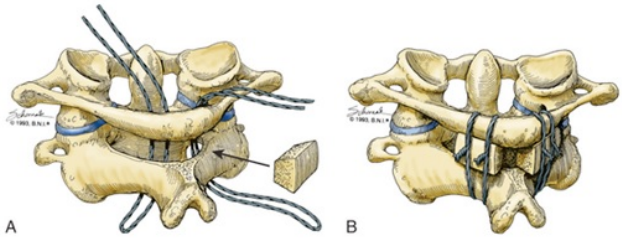


A) Loops of wire are passed using sublaminar approach at C1 and C2. Wedge shaped boned grafts are positioned bilaterally between the arches of C1-C2; B) Each graft is fixated by two wires.

Figure 3.2: Brooks-Jenkins Wiring Technique (Copyright 1993, Barrow Neurological Institute) [37]

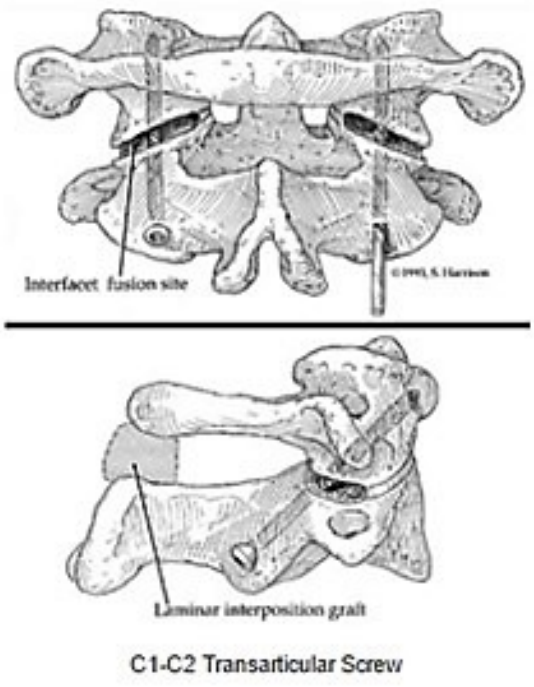


Figure 3.3: Magerl's Transarticular screw fixation [38]

Figure 3.4: Axial CT Scan of Wrights bi-lateral crossing screw fixation [36]

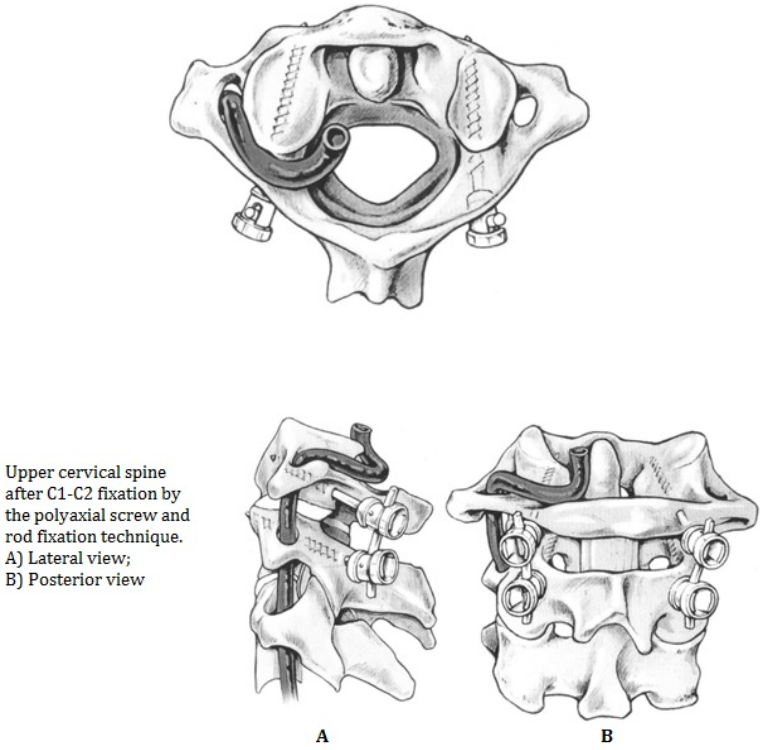


Figure 3.5: Harms and Melcher fixation [39]

### 3.1.2 C2-C7 Instrumentation

There is wide variety of instrumentation available for cervical spine (C2-C7). The type of instrumentation to be opted for surgical procedure depends on the type of spinal disorder. Since decades fusion has been considered as an optimum treatment for spinal disorders. However, the type of fusion can be categorized into two sub categories: 1. Anterior Cervical Spine Fusion 2. Posterior Cervical Spine Fusion

#### 3.1.2.1 Anterior Cervical Fusion

Anterior cervical fusion is the most common surgical procedure and is being carried out to relieve the patients from various spinal diseases. For example, if the spinal cord is compressed anteriorly due to disc herniation or bone spur. Then, anterior cervical corpectomy fusion (ACCF) or anterior cervical discectomy (ACDF) is carried out. In these procedures, unhealthy vertebrae and disc are being taken off from the cervical spine. The cavity that is being created after the removal of damaged disc and vertebrae is filled by allograft or auto-graft. However, in recent decades it has become a common practice to fill the cavity by an implant. These implants are designed in a way to allow the bone growth between the adjacent vertebral bodies while maintaining the normal spine posture. The implants are either designed as screw-plate system or standalone. In screw-plate system, implant or graft is placed inside the cavity. Then, graft or implant is locked in its position by placing a plate on the adjacent vertebral bodies and later plate is fixed by placing the screws through the plate into the vertebrae. On the other hand, standalone implants have screws attached to it and those screws are used to place the implant in the respective cavity. In order to opt for the optimum implant for a patient, doctor can get better insights about the implant from literature.

Kandziora et al [40] compared biomechanical properties of non-expandable and expandable cages with iliac crest graft. Three different types of expandable cages

were used in the study; Anterior Distraction Device (ADD), Synex-C titanium, Synex-C Peek. Besides this one non-expandable Harms mesh titanium cage was used. Kandizora et al concluded that cages had no advantage over bone graft and none of the implants are recommended to be used as standalone devices due to low extension and rotational stability. However, adding anterior plate system increased stability significantly whereas additional posterior fixation should be considered for patients with severe rotational instability.

Since, in multi-level fusion vertebral body is removed along with intervertebral disc. Brenke et al [41] analyzed 50 patients for complications after vertebral body replacement with a mean follow up of 7.3 months. Patients had undergone ACCF with ADD cage and concluded that risk for complications increase significantly when ADD is used for multiple level fusion.

As multi-level fusion can be more challenging with patients having low bone density. Hartmann et al [42] conducted in-vitro study for bi-level corpectomy and concluded that cement augmented screw-plate system reduces ROM more than conventional instrumentation and is a better option for patients with low bone density.

Li et al [43], compared standalone Fidji Cervical Cage with titanitum cage used with anterior plate system. In this study, 86 male and 52 female patients were enrolled with a minimum follow up of 2 years. In this study Fidji Cervical Cage was implanted in 68 patients (123segments) whereas cage with plate system was implanted in 70 patients (122 segments). Li et al concluded that there was no significant difference between the performance of Fidji and plate group. However, operation time, blood loss and cost is low for Fidji as compared to plate system as well as Fidji Cervical Cage is associated with lower risk of postoperative dysphagia.

Hacker et al [44], reported prospective RCT study with a maximum follow up of 2 years on Bagby and Kuslich Cervical fusion cage (BAK/C). Higher fusion and lower rate of complications was reported for cage group compared to bone only fusion. Moreover, requirement for iliac crest bone graft was less for cage

group.

Hattau et al [45], evaluated interbody fusion rate for patients undergoing anterior cervical interbody fusion (ACIF) using PEEK cages filled with synthetic bone graft. Total of 29 patients with monosegmental instability due to cervical spine injury underwent ACIF. Hattau et al reported, rate of fusion of 86.2% and concluded that ACIF with PEEK cage filled with bone graft can be an alternate to iliac crest bone graft.

In the light of above mentioned studies we cannot generalize any implant for ACDF/ACIF/ACCF. The selection of optimum implant will differ from patient to patient. In order to compare the PEEK cage with titanium cages Zhi-Jun Li et al [46] performed meta-analysis and did not any significant difference in their performance.

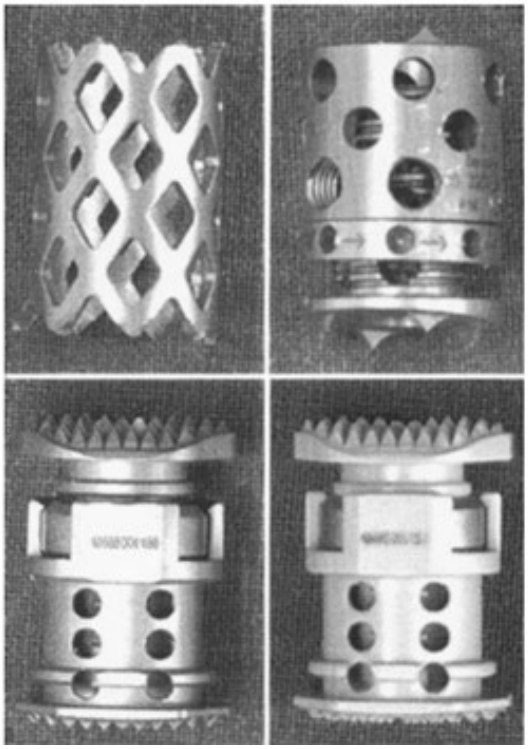

Figure 3.6: From left to the right: Harms (mesh titanium cage, non-expandable cage), ADD(expandable cage), Synex-C Titanium (expandable cage), and Synex-C PEEK (expandable cage) [40]

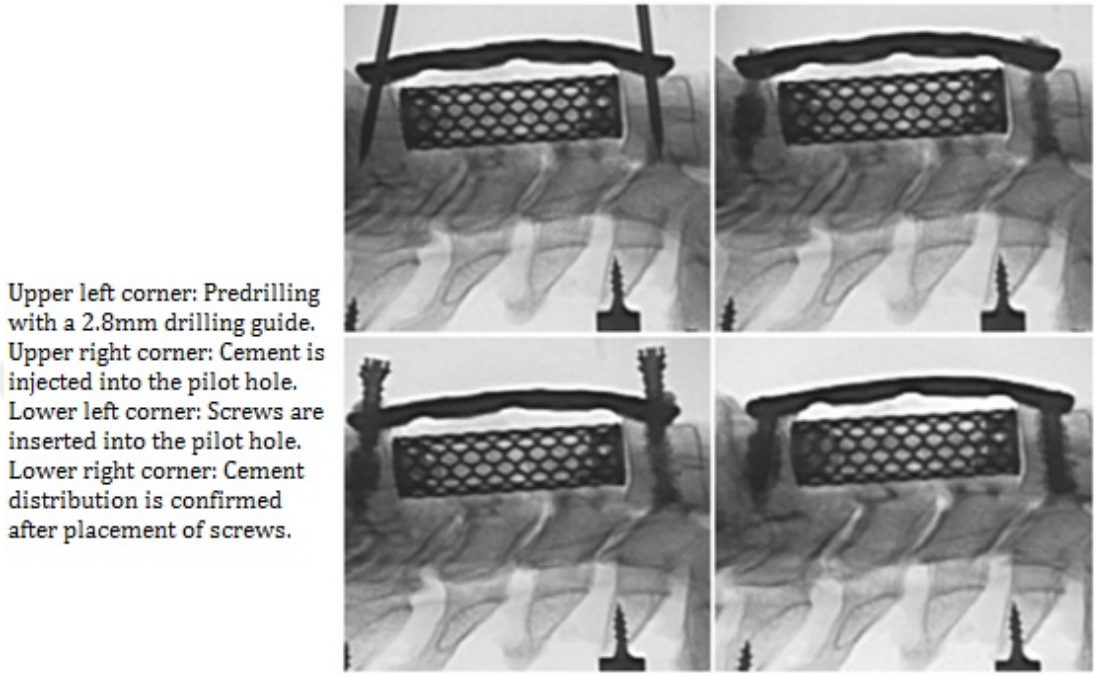


Figure 3.7: Bi-level corpectomy with cement augment screw-plate system [42]

Figure 3.8: Fidji cervical cage [43]

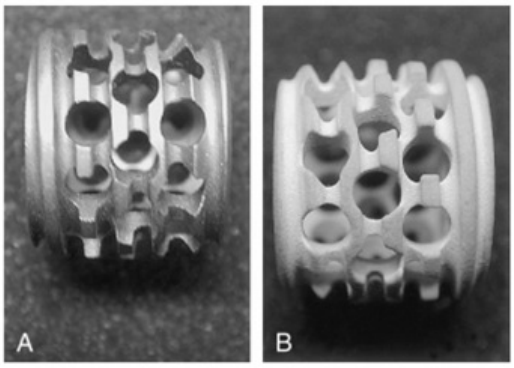


Figure 3.9: The Badby and Kuslich (BAK/C) interbody fusion cage, A) Uncoated; B) Coated with hydroxyapatite [44]

Figure 3.10: PolyEtherEtherKetone cage filled with synthetic bone graft [45]

#### 3.1.2.2 Posterior Cervical Fusion

The Posterior cervical fusion (PCF) for C2-C7 is usually carried out for laminectomy surgical procedure or when the spinous process is incompetent [47]. In PCF, the unhealthy vertebrae or disc is approached posteriorly. The screw-plate and screw-rods are common instruments used for fusing the spinal segments in PCF. Moreover, screw-rod implants are now being used in almost every cervical spine surgery. The benefit of using screw-rod implants over screw-plate implants is that they provide desirable stability and are compact at the same time. Over the time great advancements have been seen in screw design and currently polyaxial screws are used in almost every spinal fusion as they make the placement of rod easier as well as maintain the natural lordotic curvature of spine. Moreover, the bone grafts in PCF are placed sideways to the rod or plate implant used. Bone graft facilitates the bone healing at the spinal segments and eventually the spinal segments are fused together and provide stability to the spine.

PCF for C2-C7 is usually done by cervical pedicle screw, pars screw, lateral mass screw or combination of them. Pars screws are similar to the pedicle screws and the major difference is of the insertion angle. In literature we see that all implants provide acceptable results for fusion. Kim et al [48] performed PCF using polyaxial screws and implanted 486 screws in 65 patients. Among 65 patients, 1 case of dural tearing and 2 cases of lateral mass fracture were reported. However, no infection or hardware failures were reported and no patient had neurological deterioration after surgery. Kim et al concluded that polyaxial screw-rod system can be used as primary or additional fusion method in risky regions. Pedicle screw fixation gets challenging for lower cervical and upper thoracic as the size of pedicle gets small and there is risk of neurovascular injury.

After implant fixation, the major point of concern is the graft resorption rate. Lee et al [49] analyzed graft resorption and fusion rate after cervical pedicle screw fixation with a follow up of 1 year. Different graft materials were used such as; local bone, allograft and mix. The rate of fusion using cervical pedicle screw was promising as Lee et al reported 98.2% rate of fusion.

Implant failure is one of the most common problem seen in spinal fusion. Implant failure cases are seen for CPS as well as lateral mass screw. For that reason Johnston et al [50], did an in-vitro experimental study to measure fatigue and pull out strength for CPS and lateral mass screw. The cadaver study of Johnston et al concluded that pedicle screws have low screw loosening rate as compared to lateral mass screws.

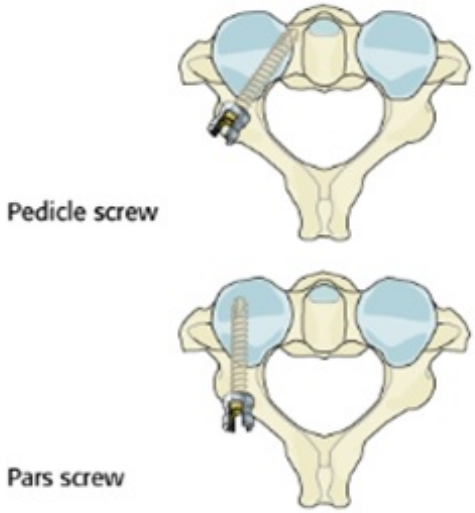


Figure 3.11: Pedicle and Pars Screw [51]

Figure 3.12: Cervical Pedicle Screw with Rod [52]

#### 3.1.2.3 Dynamic Stabilization Systems

The above mentioned fusion technique has served as a gold standard for stabilizing cervical spine but in recent decades its reliability has become questionable

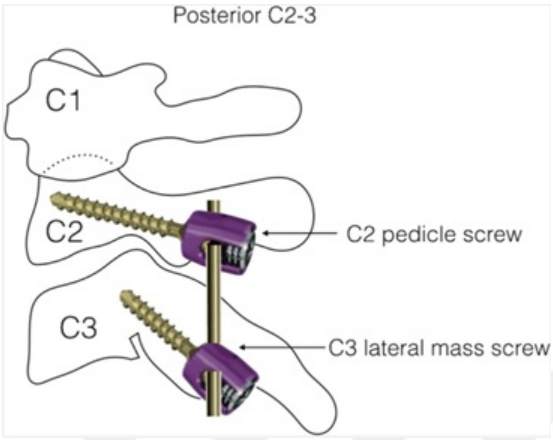


Figure 3.13: Lateral view of C2 pedicle and C3 lateral mass screw fixation [53]

due to its postoperative effects. Since fusing the spinal segment results in loss of motion at the index segment. Hence that loss is compensated by the adjacent segments and this phenomenon is termed as adjacent level effect (ALE). To overcome the adjacent level effects, dynamic stabilization systems are being proposed by medical professionals. During the recent decades, dynamic stabilization systems have become increasingly popular and are replacing the old fusion technique. In cervical spine, total disc replacement (TDR) surgery is performed where unhealthy disc is replaced by artificial disk. Currently, there are different types of artificial discs available. Bryan disc is one of the most commonly used disc in TDR and number its reliability has been reported in literature [54–56]. Gandhi et al [56] carried out in-vitro and finite element (FE) study on cervical spine by implementing single and bi-level TDR, fusion as well as hybrid system (fusion followed by TDR). The single and bi-level TDR was implemented using Bryans disc and Prestige LP. The TDR was done at C5-C6 segment and C6-C7 segment. Six cadaver specimens were used in his study which were examined under flexion-extension, lateral bending and axial rotation. Besides this, hybrid loading protocol was used to evaluate the effect of Bryans disc on ROM of spine. This study of Gandhi et al leaded to the conclusion that the TDRs are better in terms of preserving the motion at index level as well as they do not increase the stress at the adjacent segments as compared to fusion. Positive results for Bryans disc are also reported by Coric et al who carried out prospective randomized study with an average follow up of 6 years. Coric et al compared the outcome of Bryans

and Kineflex—C disc to ACDF. Patients with TDR showed significant increase in ROM as compared to ACDF. Moreover, Coric also mentioned in his study that 2 out of 41 TDR patients had adjacent level reoperation and 1 patient had reoperation for the index level and all the operations were laminoforaminotomies. On the other hand 1out of 33 ACDF patients had adjacent level reoperation and screw loosening was reported in 1 patient. The reliability of Bryans disc is also backed by 10 year follow up study carried out by Dejaegher et al. This follow up study was based on 72 patients and neurological improvement was seen in 89% patients. Whereas 6% of patients required adjacent level surgery. Besides this it has been reported that Bryan disc tends to alter the cervical lordotic curvature but that change in segmental kyphosis is considered clinically insignificant [57, 58].

Figure 3.14: Bryan Cervical Disc [56]

The other common artificial disc available in the market is ProDisc-C, it has been used widely and various studies have been carried out on it. Laumeau et al [59] has reported clinical outcome of RCT study with a follow up of 7 years. They compared the results of ProDiscC to ACDF for patients with single level symptomatic cervical disc disease (SCDD). Laumeau et al concluded that total ROM was maintained with TDR as well as neck and arm pain improved with TDR as compared to ACDF. Moreover 6 reoperations (4 adjacent level, 2 index level) were done for patients with ACDF whereas no reoperation was done for patients with ProDiscC implantation.

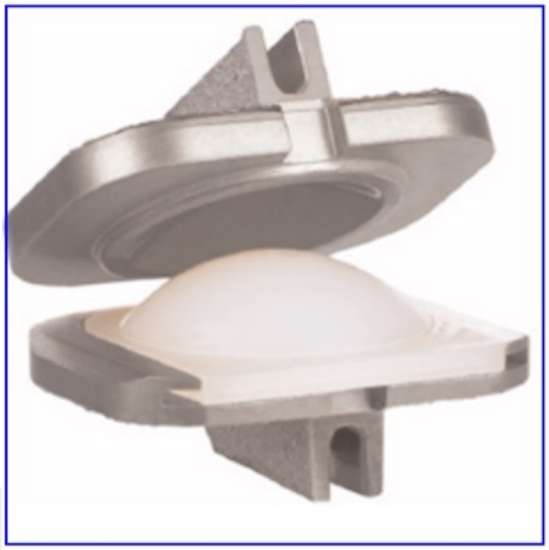

Figure 3.15: ProDisc-C cervical disc prosthesis [60]

Besides Bryans disc and ProDiscC, Prestige LP and Prestige ST cervical disc are being widely used to provide dynamic stability to the cervical spine. In order to evaluate the durability of this device, clinical studies have been done and reported by medical professionals. Gandhi et al [56] conducted a biomechanical study to do the comparasion of biomechanics of spine after TDR and fusion as described in above section for Bryans disc. His study concluded that the Prestige LP cervical disc preserves the motion at the index level and it requires less hybrid moment to achieve the total ROM of the intact spine as compared to Bryans disc. On the other hand, RCT studies have been reported for Prestige ST [61–63]. Mummaneni et al carried out RCT study with a follow up of 2 years. In this study 541 patients were enrolled, out of which 223 patients with TDR completed the 2 year follow up and 198 patients with ACDF completed the follow up. After 2 years of follow up mummaneni et al concluded that Prestige ST maintained the physiological ROM better and there were less reoperations for TDR as compared to ACDF. Later, the follow up of this study was increased to 5 and 7 years and the TDR still proved to be better option than the ACDF [61, 63].

By reviewing the literature, we can deduce that the artificial disks perform better than ACDF in terms of preserving motion at index level and reducing adjacent segment degeneration. The patients with TDA have less chances of having

Figure 3.16: Prestige ST and Prestige LP [56]

secondary surgery. In order to diminish the chances of secondary surgery medical professionals are working day and night to come up with optimum solution for cervical spine instability. Therefore, we see number of devices available in market such as Mobi-C Cervical Disc, PCM Cervical Disc, Secure-C etc. The clinically significant outcome of these discs is also reported in literature [64–66].

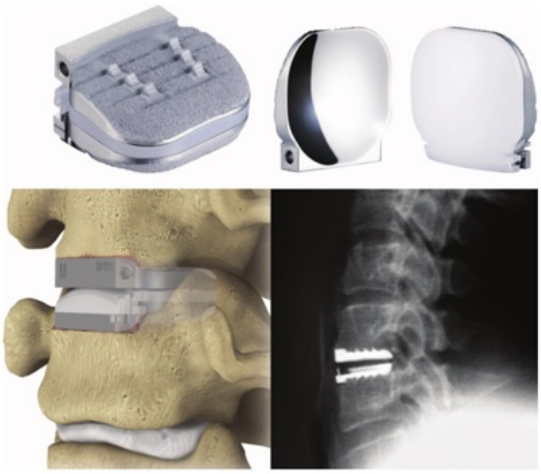

Figure 3.17: PCM Cervical Disc [66]

Clock-wise from upper Left: The assembled disc, disc components, neutral lateral radiograph of the disc in position, and illustration of the disc in position.

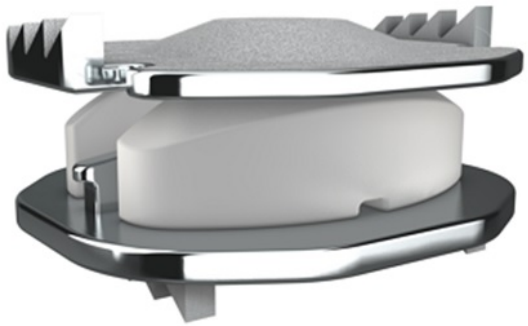

Figure 3.18: Mobi-C Cervical Disc [67]

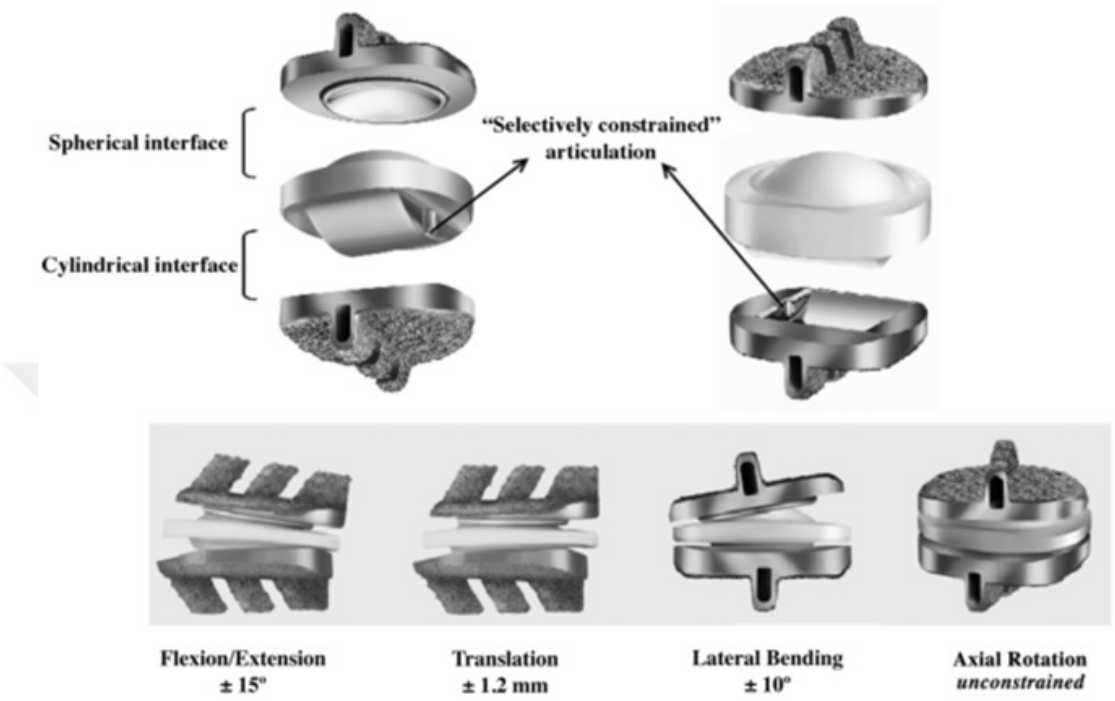


Figure 3.19: SECURE-C [64]

# Chapter 4

# FE model of atlantoaxial junction (C0-C2)

## 4.1 Intact FE Model

A three-dimensional (3-D) FE model was developed for the upper cervical spine (C0-C1-C2). Computerized tomographic (CT) scans of a 35-year-old male were used for precise construction of the geometry of the bones. The CT scan data were processed using the MIMICS (Mimics Version 14.1; Materialise, Inc., Leuven, Belgium) software to generate 3-D surfaces of the bones. The 3-D geometry of the bones was meshed using the IA-FE MESH (University of Iowa, IA, USA) software. Hexahedral elements were used to mesh the C1 and C2 vertebrae, whereas the skull was meshed using tetrahedral elements. The meshed vertebrae and skull were imported into ABAQUS (ABAQUS, Version 6.10-2; Abaqus, Inc., Providence, RI, USA) and combined with material properties inputs for the FE analysis (Figure 4.1). The bones were simulated as isotropic linear elastic materials, with different property values assigned to the cortical and cancellous bones. For the skull, the cortical bone material properties were used (Table 4.1).

Table 4.1: Mechanical properties and element types of the different parts of the cervical spine model

| Component | | | | |
|---|---|---|---|---|
| Bony Structure | Element Type | Young's Modulus (MPa) | Poisson's Ratio | Cross-Sectional Area (mm2) |
| Vertebral Cortical Bone | Isotropic, elastic hex element | 10,000 | 0.30 | - |
| Vertebral Cancellous Bone | Isotropic, elastic hex element | 450 | 0.25 | - |
| Ligaments | | | | |
| Transverse, Tectorial Membrane | Isotropic, elastic hex element | 80 | 0.3 | - |
| Apical-Alar | Tension only, truss elements | 20 | 0.3 | - |
| Anterior Longitudinal | Tension only, truss elements | 15 (12%) 30 (12%) | 0.3 | 11.1 |
| Posterior Longitudinal | Tension only, truss elements | 10 (12%) 20 (12%) | 0.3 | 11.3 |
| Ligamentum Flavum | Tension only, truss elements | 5 (25%) 10 (25%) | 0.3 | 46.0 |
| Capsular | Tension only, truss elements | 7 (30%) 30 (12%) | 0.3 | 42.2 |
| Joint | | | | |
| Facet (Apophyseal Joint) | Nonlinear soft contact, GAPUNI | - | - | - |

All of the major ligaments contributing to stabilization of the joint were modeled with different types of elements. The transverse ligament and tectorial membrane were modeled as a 3-D structure in Solidworks (SOLIDWORKS, Version 2013; SolidWorks Corp. Concord, MA, USA), based on geometry information available in the literature, and were defined as isotropic linear elastic materials. The alar ligament, apical ligament, anterior atlantoaxial ligament, anterior longitudinal ligament, posterior longitudinal ligament, ligamentum flavum, capsular ligament, and interspinous ligament were represented by tension-only truss elements, with cross-sectional areas obtained from the literature [68]. Contact at the facet joints was simulated using nonlinear GAPUNI elements. Surface-to-surface finite sliding contact was permitted between the transverse ligament and the odontoid process.

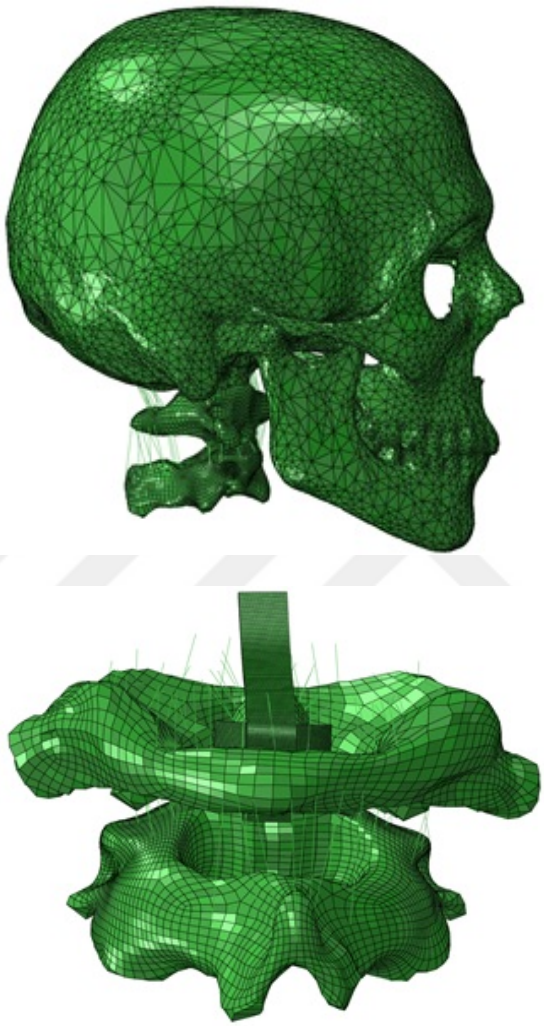

Figure 4.1: FE model of the upper cervical spine

## 4.2 Injured and Implanted FE Models

Three screw-based constructs were modeled in Solidworks: (1) C2 with a transarticular screw (C1-C2TA), (2) C1 with a lateral mass screw and C2 with a pedicle screw (C1LM-C2PD), and (3) C1 with a lateral mass screw and C2 with a translaminar screw (C1LM-C2TL). All of the screws were 4 mm in diameter. The diameter of the connecting rod was 3.5 mm. A type II dens fracture was induced in the intact FE model to create an injured FE model. The screw constructs were added to the intact and injured FE models. Three groups of FE models were simulated under similar loading conditions: 1- Intact 2- Implanted intact 3-

Implanted injured The interfaces between the screw and the bone and between the screw head and the rod were constrained in all directions using the coupling option in ABAQUS. Titanium material properties were assigned to the screws and rods.

## 4.3 Loads and Boundary Conditions

The lower surface of the C2 vertebra was constrained in all directions. A 1.5-Nm pure moment was applied in the three main planes: flexionextension (FLEX), rightleft lateral bending (LB), and rightleft axial rotation (AR). In each case, the pure moment was applied to a flying node that was coupled to the surface of the condyles.

The intact model was used in the FE simulation to predict the ROM of the C0-C1 and C1-C2 segments, and the results were compared with values reported in the literature. The implanted intact and implanted injured FE models were then used in the simulation. The maximum von Misses stresses in the different implants under the different loading conditions were compared.

## 4.4 Results

### 4.4.1 Model Validation

The ROM predicted using the intact FE model was compared to the ROM reported by Panjabi et al. [69–71] (Table 4.2). The FE model predictions were largely within the reported range for every loading condition, with very small deviations observed for C0-C1 during flexion and for C1-C2 during extension and lateral bending.

Table 4.2: Comparison between predicted ROM (degrees) of the C0-C1 and C1-C2 segments according to FE model and reported ROM in in vitro studies by Panjabi et al.

| Load Case | Segment | Panjabi et al. [] | Panjabi and Myers [] | Our FE model |
|---|---|---|---|---|
| **Flexion** | C0-C1 | 10.8-17.2 | - | 8.6 |
| | C1-C2 | 9.8-16.2 | - | 10.8 |
| **Extension** | C0-C1 | 10.8-17.2 | - | 13.6 |
| | C1-C2 | 6.0-16.0 | - | 19.6 |
| **FlexionExtension** | C0-C1 | - | 24.5 (4.0) | 22.2 |
| | C1-C2 | - | 22.4 (4.7) | 30.4 |
| **Lateral Bending** | C0-C1 | 2.6-8.6 | 5.5 (2.5) | 5.9 |
| | C1-C2 | 3.8-19.6 | 6.7 (4.4) | 2.5 |
| **Axial Rotation** | C0-C1 | 1.0-10.5 | 7.3 (2.2) | 10.6 |
| | C1-C2 | 24.2-46.4 | 38.9 (5.4) | 25.9 |

### 4.4.2 Implanted Model

The ROM reduction of the C1-C2 segment after the addition of the three constructs to the intact and the injured models was measured and normalized with respect to the intact ROM (Table 4.3). In FLEX, the C1-C2TA construct reduced the ROM by 99% for both the intact and the injured model. The C1LM-C2PD and C1LM-C2TL constructs achieved similar ROM reductions (98%) when added to the intact model and ROM reductions of 96% and 95%, respectively, when added to the injured model.

In LB, the C1-C2TA construct reduced the ROM by 98% and 100% for the intact and injured models, respectively. The C1LM-C2PD construct only reduced the ROM by 93% for the intact model but reduced the ROM by 95% when added to the injured model. The C1LM-C2TL construct reduce the ROM much less than the other two techniquesby 75% and 74% for the intact and the injured models, respectively.

In AR, the C1-C2TA construct reduced the ROM by 99% for both the intact and injured models. The C1LM-C2PD construct reduced the ROM by 98%. Compared to the intact model, the C1LM-C2TL construct increased the stiffness when added to the injured model, achieving a 98% ROM reduction for the intact

model and 99% reduction for the injured model.

Table 4.3: Comparison between intact ROM reduction (degrees) in the C1-C2 segment after adding the three-screw construct to both the intact and injured models. Normalized values are shown in parentheses.

| | Intact | C1-C2TA (Intact) | C1-C2TA (Injured) | C1LM-C2PD (Intact) | C1LM-C2PD (Injured) | C1LM-C2TL (Intact) | C1LM-C2TL (Injured) |
|---|---|---|---|---|---|---|---|
| **FLEX** | 30.4 | 0.25 | 0.2 | 0.48 | 1.32 | 0.16 | 0.12 |
| | | -99% | -99% | -98% | -96% | -98% | -95% |
| **LB** | 2.5 | 0.05 | 0 | 0.16 | 0.12 | 0.61 | 0.64 |
| | | -98% | -100% | -93% | -95% | -75% | -74% |
| **AR** | 25.85 | 0.09 | 0.06 | 0.27 | 0.24 | 0.39 | 0.48 |
| | | -99% | -99% | -98% | -98% | -98% | -99% |

### 4.4.3 Stresses in Implants

A comparison of the predicted maximum von Mises stresses in the three screw constructs is shown in Figure 4.5. The largest predicted maximum stress for the C1-C2TA construct was 133 MPa when the construct was added to the injured FE model and occurred in FLEX. The location of the maximum stress was the point at which the screw entered C1.

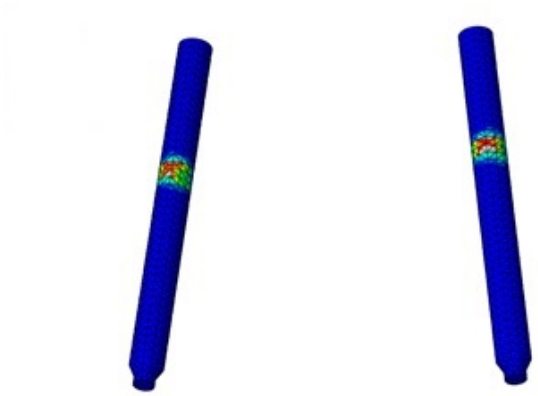

Figure 4.2: Stress in C1-C2TA

The largest predicted maximum stress for the C1LM-C2PD construct was 307 MPa in FLEX. The location of the maximum stress was the lateral mass screw head. In the pedicle screw, the maximum stress was 131 MPa.

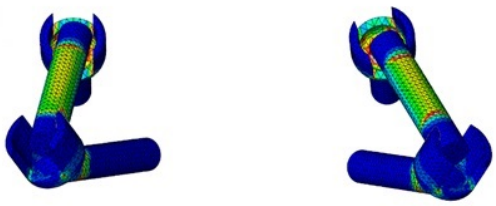

Figure 4.3: Stress in C1LM-C2PD

The largest predicted maximum stress for the C1LM-C2TL construct was 332 MPa in FLEX. The location of the maximum stress was the lateral mass screw head similar to the C1LM-C2PD construct. In the translaminar screw, the maximum stress was 123 MPa.

Figure 4.4: Stress in C1LM-C2TL

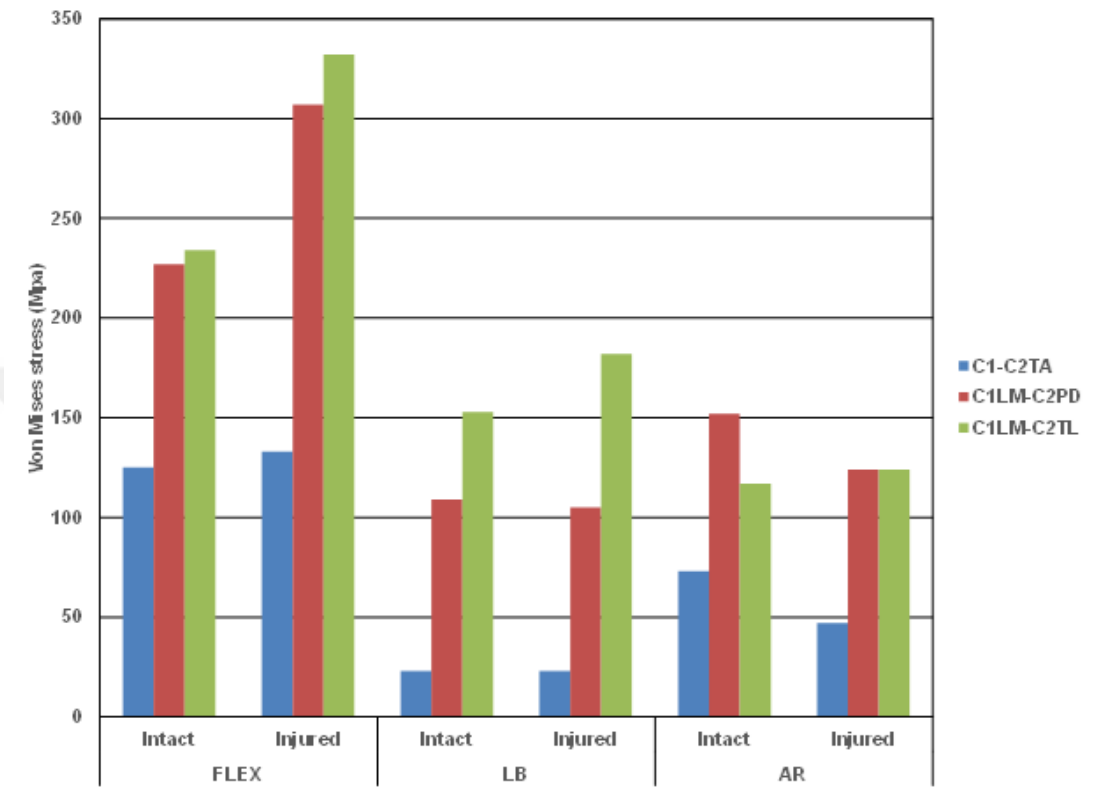


Figure 4.5: Maximum stress in the construct during FLEX, LB, and AR for both the intact and injured models

## 4.5 Discussion

Odontoidectomy in the form of a Type II dens fracture was added to the intact FE model to destabilize the joint. This type of fracture is one of the most common indications for surgery using atlantoaxial fixation techniques [72].

Our FE study showed that the three screw constructs reduced the C1-C2 segment ROM significantly in all loading directions, except the C1LM-C2TL construct in LB. The C1LM-C2TL screw construct in LB achieved a 74% ROM reduction, which was much less than the reductions achieved by the other two screw constructs. This finding is consistent with the findings of other biomechanical studies. Lehman et al. [73] found that the translaminar screw construct did not reduce the ROM significantly in LB and AR after odontoidectomy, compared

to the pedicle screw construct. Similarly, Lapsiwala et al. [74] reported the weakness of the translaminar screw construct in ROM reduction of the atlantoaxial joint in LB compared to the transarticular and pedicle screw constructs. However, Gorek et al. [75] did not report a significant difference in ROM reduction between the translaminar and pedicle screw constructs. Interestingly, Dorward and Wright [72] (the same Wright who was the first to use the translaminar construct in atlantoaxial fixation) believe that the lower stiffness of the atlantoaxial joint after addition of a translaminar screw construct does not prove the superiority of the transarticular and the pedicle screw constructs. We however believe that the lower biomechanical stability of the joint that results from adding the translaminar screw construct can cause failure in the construct due to fatigue. More importantly, the high mobility of the upper cervical region subjects the construct to extensive cyclic loading. The maximum stresses in the C1LM-C2PD and C1LM-C2TL screw constructs were 56% and 59% higher, respectively, than the maximum stress in the C1-C2TA screw construct. The reason for the significant differences in the maximum stress between the screw constructs may be related to the cantilever concept on which the design of the C1LM-C2PD and C1LM-C2TL screw constructs is based. Although these two constructs are known to be less challenging atlantoaxial fixation techniques in surgery than the C1-C2TA construct, they are more prone to failure because of the higher stresses induced.

## 4.6 Conclusion

Our model indicates that translaminar screws are not as reliable as transarticular and pedicle screws in term of biomechanical stability of the atlantoaxial joint in lateral bending. Translaminar screws produce larger stresses that may lead to failure of the construct before the required bony fusion occurs in the segment.

# Chapter 5

# FE Model of Cervical Spine (C2-C7)

## 5.1 Intact and Implanted FE models

The validated three dimensional FE model of intact cervical spine from C2-C7 was used in this study as shown in Figure 5.1. This model has been validated against the literature and in-vitro studies in our previous study [76]. The model was previously constructed by using the computer tomographic images of a 35-year-old male. For studying the effects of DCI implant on the cervical spine, the model was manipulated accordingly. In the first place the geometry of the DCI implant was obtained from the literature and it was modeled in SolidWorks. After creating the solid model of DCI implant in SolidWorks it was exported to ABAQUS software (ABAQUS, Version 6.10-2; Abaqus, Inc., Providence, RI, USA) and was meshed using the tetrahedral elements as shown in Fig. 3. The implant was given material property of a Titanium Alloy (Ti6Al4V) with a young modulus of 114,000MPa and a poissons ratio of 0.35. Finally, the meshed implant was placed at the desired index segments by coupling upper surface of the implant with superior segment and coupling the lower surface of the implant with the inferior segment. For simulating the single level disc replacement, disc between the segment C5-C6

was removed along with the ligaments i.e. anterior longitudinal ligament (ALL) and posterior longitudinal ligament (PLL), in order to create a cavity for the implant to be placed and mimic the real surgery scenario. Similarly, bi-level disc replacement was simulated by removing the discs and ligaments between segments C4-C6. In order to simulate hybrid surgery (HS), disc between the C5-C6 segment was replaced by implant whereas C4-C5 segment was fused by removing the ALL and PLL whereas disc C45 was assigned the material property of cancellous bone. Similarly, single and bi-level fusion was simulated by fusing C5-C6 segment and C4-C6 segments by assigning cancellous bone property to the discs C56 and C46 respectively.

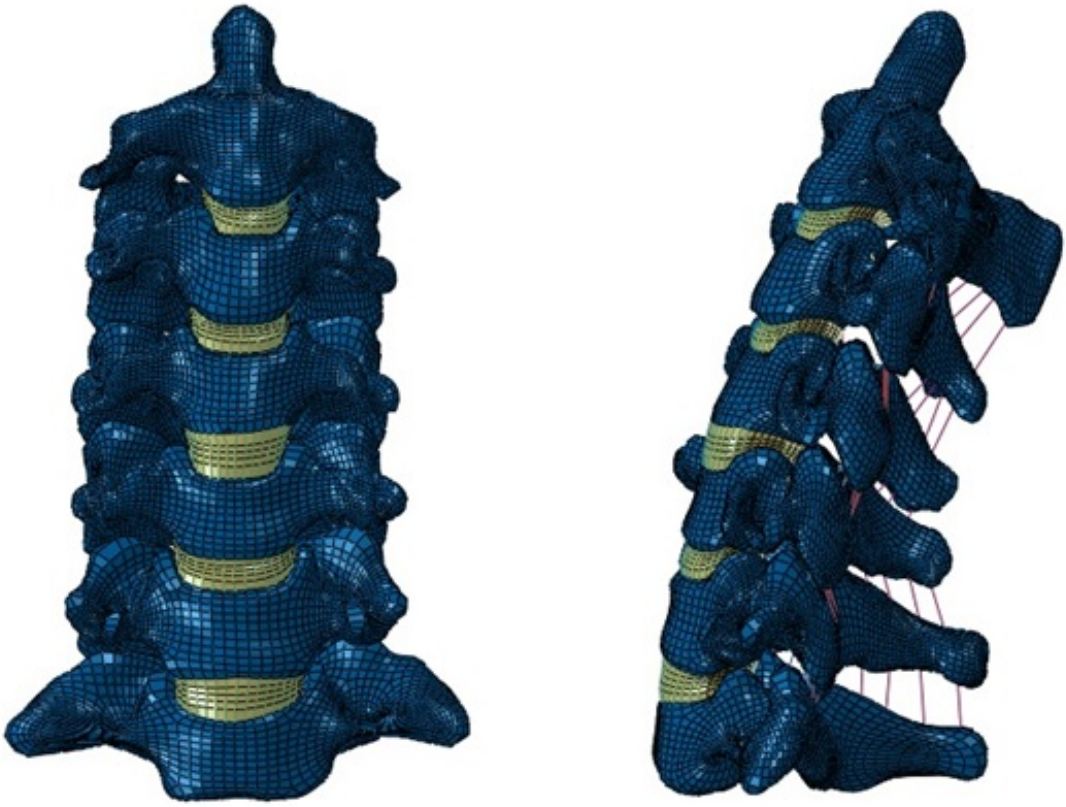

Figure 5.1: FE model of intact C2-C7 cervical spine

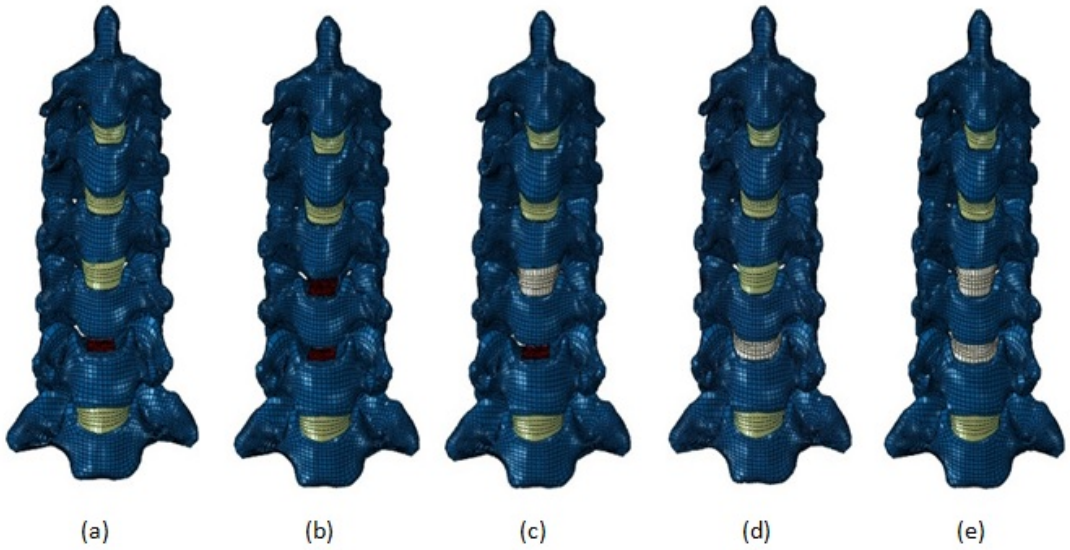


Figure 5.2: a) C5-C6 DCI model, b) C4-C6 DCI model, c) Hybrid model, d) C5-C6 fused model, e) C4-C6 fused model

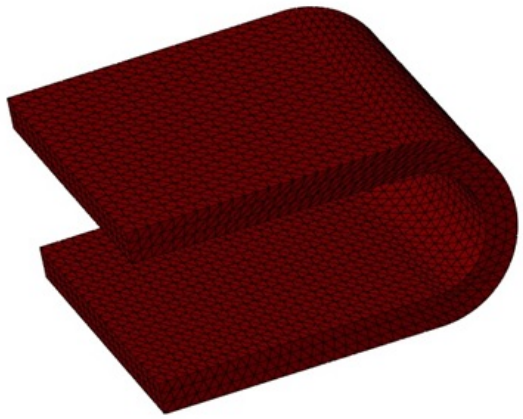

Figure 5.3: U-Shaped Dynamic Cervical Implant (DCI)

## 5.2 Loads and Boundary Conditions

The pure bending moment was applied in three planes sagittal, coronal and axial. The reference point for applying the moment was created 2mm above the odontoid process and coupled with the top surface of odontoid i.e. C2, whereas the bottom surface of the vertebrae C7 was constrained in all the simulations.

The model was tested under 2 Nm pure moment applied in either direction of flexion-extension, lateral bending (LB) and axial rotation (AR). ROM for each segment was calculated and compared with the results of intact spine. After obtaining the FE solutions for all the models, the post processing of data obtained from ABAQUS was done in MATLAB by writing custom scripts.

## 5.3 Results

### 5.3.1 Range of Motion

The ROM for all the models is calculated against the intact model with the following formula:

ROM Deviation=(Implanted-Intact)/Intact*100

The ROM was reduced about 38% at C5-C6 segment in C5-C6 DCI, C4-C6 DCI and Hybrid-DCI during flexion. Whereas the ROM was reduced about 5.9% at C4-C5 segment in C4-C6 DCI model. During extension the maximum increase in ROM of 42% was seen at index segment in Hybrid-DCI model and about 39.7% increase in ROM was seen in C5-C6 DCI and C4-C6 DCI. Moreover, the ROM at C4-C6 segment was increased by 39.67% in C4-C6-DCI model. Besides this, adjacent segments were least affected during flexion and the deviation was less than 1% in all the models including the fusion models. However, adjacent segments were affected significantly during extension and the maximum increase in ROM of about 8.71% was seen in C4-C6 Fused model at the superior segment. Whereas reduction of 1.35% and 3.87% was seen at superior segment in C5-C6 DCI and C4-C6 DCI model respectively. On the other hand, Hybrid-DCI model had 2.56% increase in ROM at the superior segment.

The reduction in ROM during LB increased significantly, where C4-C6 DCI model had 66.6% and 83.70% reduction in ROM at C4-C5 and C5-C6 segment respectively. Besides the 84.25% and 85.39% reduction in ROM was observed at

C5-C6 segment in C5-C6 DCI and Hybrid-DCI model respectively. Beside this, increase in ROM was observed at adjacent segments in all the models whereas the maximum increase in ROM was seen at the superior segment of C4-C6 Fused model i.e. 11.35%. Moreover, 10.28% increase in ROM at the superior segment in Hybrid model was seen. The C5-C6 DCI model had only 0.25% increase in ROM at the superior segment.

During AR about 89% reduction in ROM was observed in all the implanted models at C5-C6 segment, whereas C4-C5 segment in C4-C6 DCI model had 79.42% reduction in ROM. On the other hand, increase in ROM was seen at the adjacent segments of all the model but the C2-C3 segment had a decrease in ROM in all the models unlike flexion/extension and LB. The superior segment in C5-C6 DCI and C5-C6 Fused had increase in ROM of 5.92% and 6.34% respectively. Besides this, adjacent segments in other models had less than 4% increase in ROM.

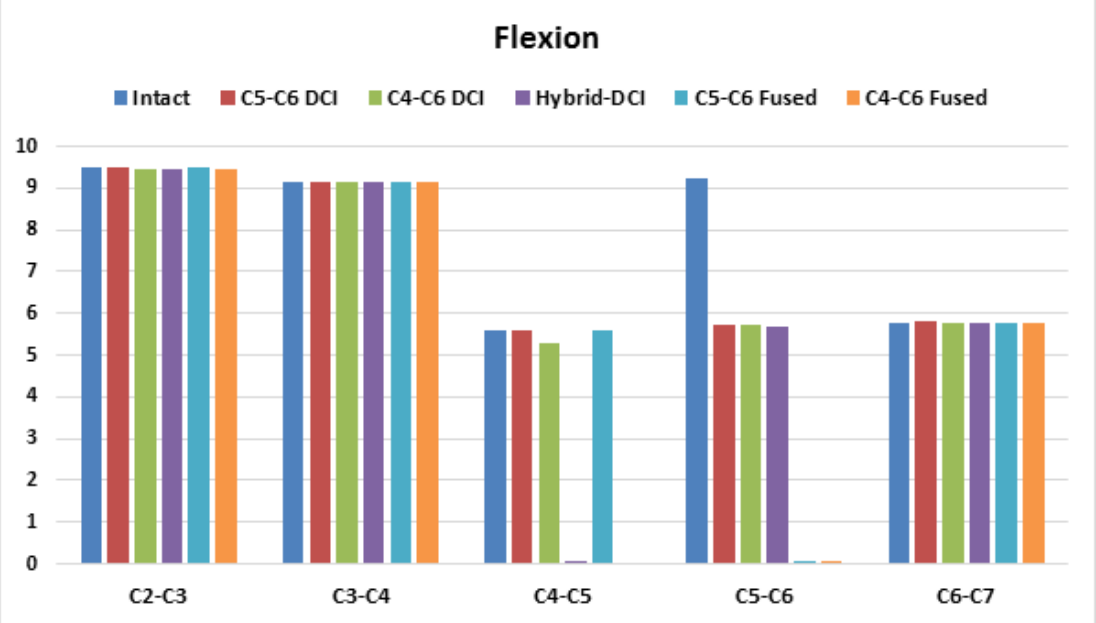


Figure 5.4: The comparison of ROM under flexion among C5-C6 DCI, C4-C6 DCI, Hybrid-DCI, C5-C6 Fused, and C4-C6-Fused model

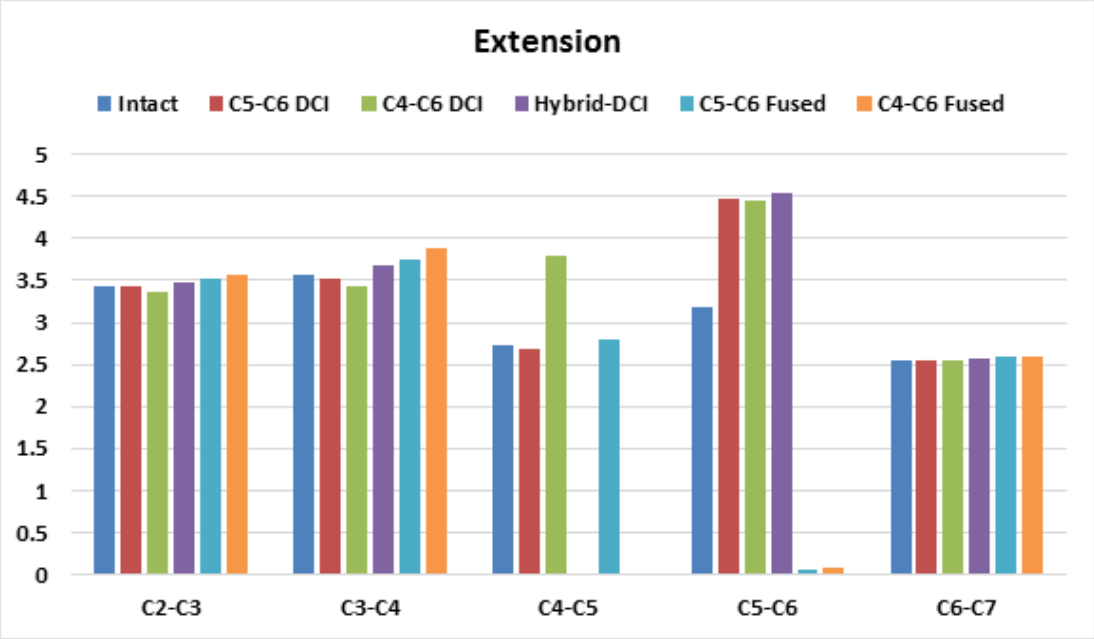


Figure 5.5: The comparison of ROM under extension among C5-C6 DCI, C4-C6 DCI, Hybrid-DCI, C5-C6 Fused, and C4-C6-Fused model

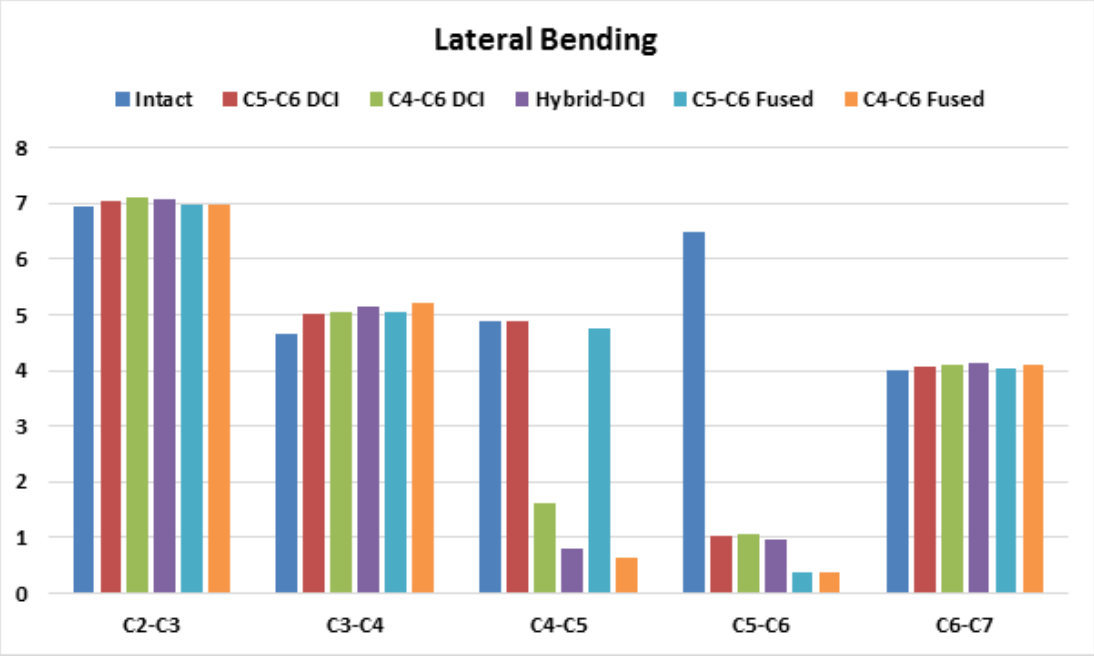


Figure 5.6: The comparison of ROM under lateral bending among C5-C6 DCI, C4-C6 DCI, Hybrid-DCI, C5-C6 Fused, and C4-C6-Fused model

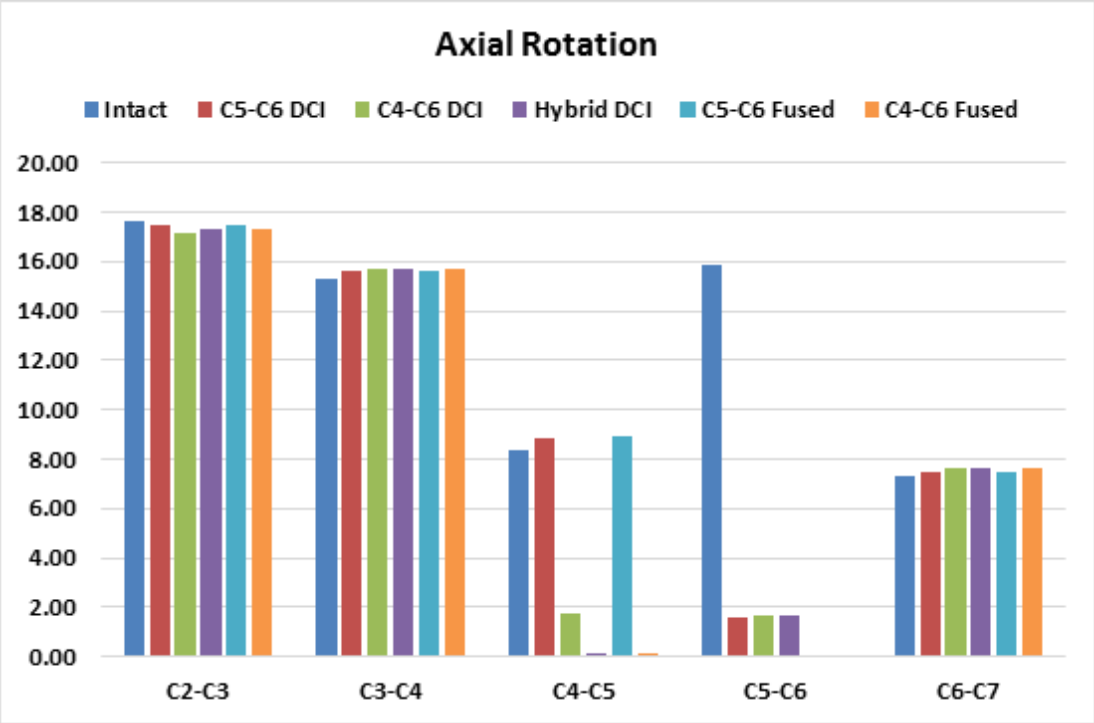


Figure 5.7: The comparison of ROM under axial rotation among C5-C6 DCI, C4-C6 DCI, Hybrid-DCI, C5-C6 Fused, and C4-C6-Fused model

### 5.3.2 Stress Distribution in Implant

The maximum von Mises stress predicted in the implant for different models are summarized in Fig. 5.8. The maximum stress was seen during flexion in all the models and it was highest in C4-C6 DCI i.e. 765.85 MPa at C5-C6 segment. During the extension maximum stress of 633.64 MPa was predicted in Hybrid-DCI model. For LB the maximum stress of 575.62 MPa was predicted during the right lateral bending (RLB) at C4-C5 segment of C4-C6 DCI model. Moreover, stress in the implant during right axial rotation (RAR) was about 648.5 MPa at C5-C6 and C4-C6 segment of C5-C6 DCI and C4-C6 DCI respectively.

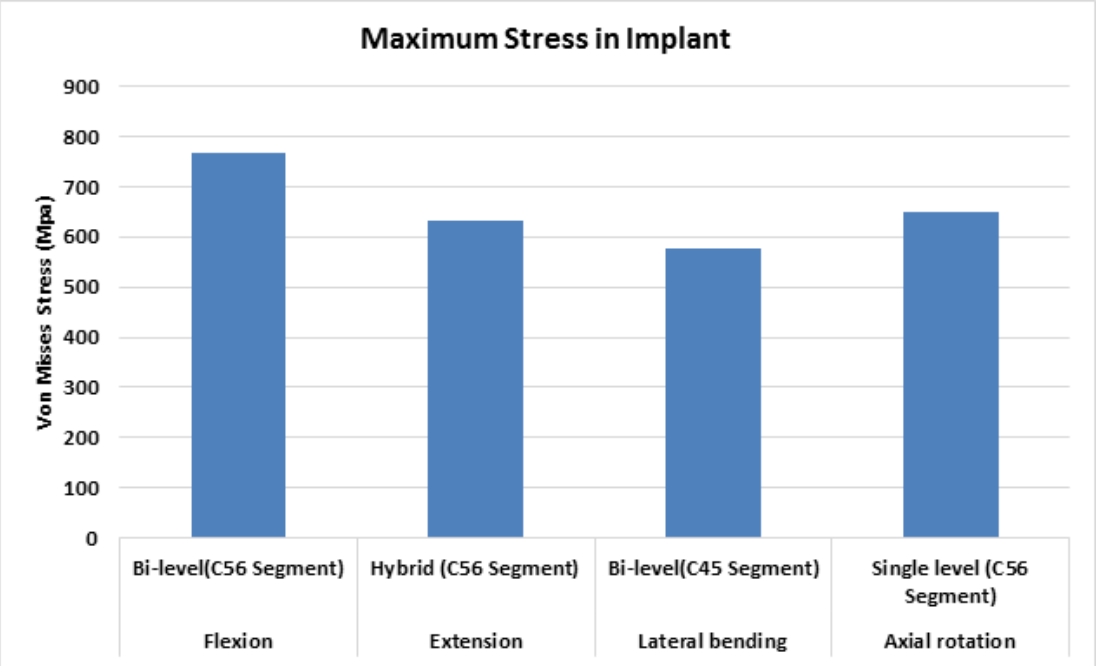


Figure 5.8: Maximum stress in the implant during flexion, extension, lateral bending, and axial rotation

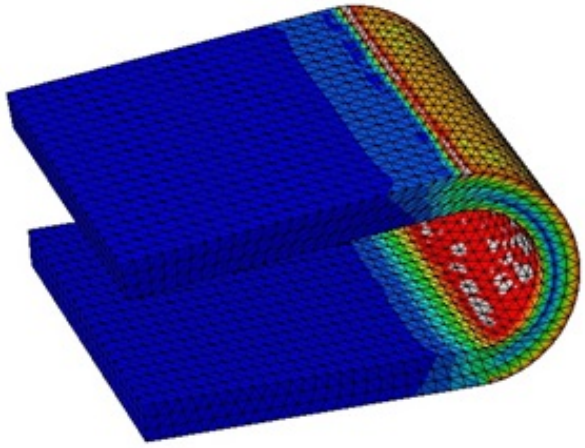

Figure 5.9: Maximum stress distribution in U-Shaped Implant (DCI) during flexion in C4-C6 DCI model

## 5.4 Discussion

Our FE results showed that the DCI implant in all the models causes reduction of ROM at the index segment during flexion and increases the ROM during extension and the similar trend has been reported by Li et al [77]. Besides this DCI implant did not result in significant increase of ROM at the adjacent segments like C4-C6 Fused model where adjacent segments ROM was increased up to 8.7% compared to intact model. Moreover, our FE results showed that the DCI implant reduces ROM significantly during LB and AR at the operated segment. In LB the maximum deviation at the adjacent segment was seen for Hybrid-DCI model compared to C5-C6 DCI and C4-C6 DCI. The interesting point to note in C5-C6 DCI model is that C3-C4 segment is more affected compared to adjacent segments C4-C5 and C6-C7. During LB the increase in ROM of C3-C4 segment of DCI model is up to 7.5% whereas the increase in ROM of adjacent segments is less than 2% and a similar trend has been reported by Zhong et al [78]. However, in AR the superior adjacent segments ROM was increased more in C5-C6 DCI compared to C4-C6 DCI and Hybrid-DCI model. The results for ROM using DCI implant show that it prevents rotation greatly and our findings are consistent with the prospective case study of Mohamed et al. [79]31. Since, the shape of

DCI implant permits flexion/extension moment. Therefore, maximum von Mises stress is also predicted during flexion in all the implanted models and our finding is in confirmation with other FE studies [77, 78].

## 5.5 Conclusion

Our biomechanical FE study showed that the DCI implant is a good alternate to ACDF but it has its own limitations. The DCI implant shows reasonably well results for flexion/extension but the stress in implant is also maximum in flexion. The ROM of adjacent segments is least affected in C5-C6 DCI model. Whereas, deviation in ROM of adjacent segments is maximum for Hybrid-DCI model. Besides this DCI implant tends to experience high stress in bi-level disc replacement model as compared to single and hybrid disc replacement model.

# Chapter 6

# FE Model of Knee Joint

## Model Development

This section discusses the method and approaches used to obtain the geometry of hard tissues as well as soft tissues. The approach used for making soft tissues is a novelty of this project. Besides soft tissues, this chapter also discusses the method for development of tendons for applying muscle loads. Lastly, all the parts of knee joint structures were meshed in IA-FE MESH.

The process of model development is sub divided into 3 categories:
Development of bones geometry from CT scans.
Development of soft tissues using CAD.
Development of Tendons

## 6.1 Development of Bones Geometry

The computerized tomography (CT) scans were used to obtain the geometry of bones. The bones were masked in MIMICS in order to get the 3D geometry of

bones. However, after having considerably good shape of the bones they were smoothed to eliminate the sharp edges present at the surface of bones.

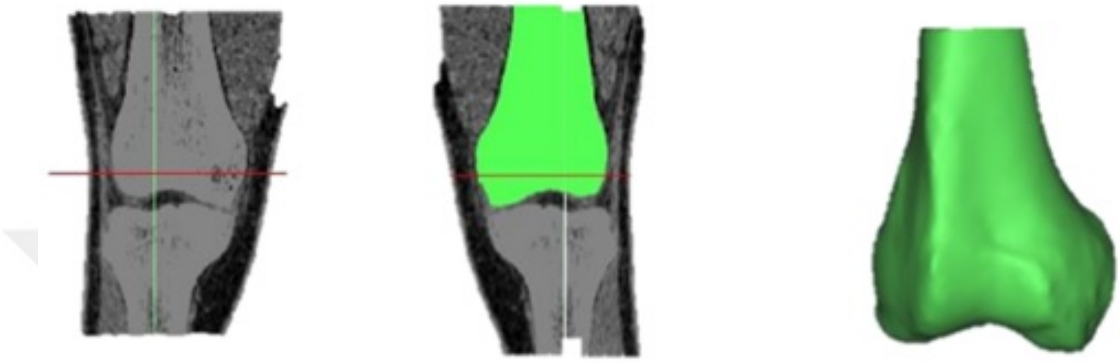

Figure 6.1: Masking of Femur in MIMICS

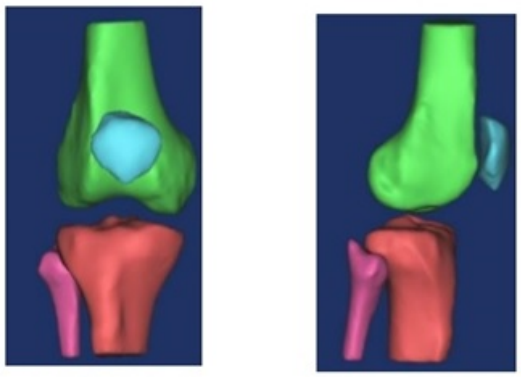

Figure 6.2: Geometry of knee joint obtained in MIMICS

## 6.2 Development of Soft Tissues

The geometry of soft tissues was toughest to obtain since they do not appear clearly in the CT scans. Moreover, cruciate ligaments appear to be overlapping over each other. So, for that reason scans could not be used to construct ligaments 3D Geometry. In this study anterior cruciate ligament (ACL), posterior cruciate ligament (PCL), medial collateral ligament (MCL) and lateral collateral

ligament (LCL) were represented by 3D geometry and their geometry was obtained from literature [80–86]. However, other ligaments such as Post. Capsule Lateral, Post. Capsule Medial, Post. Capsule Oblique and Post. Capsule Arcuate were represented using truss elements and their attachment on femur and tibia was obtained from literature [87]. Meniscus and Cartilages were also represented as 3D structures. The development of cartilage and meniscus was slightly different than the ligaments and is described in detailed in the next section:

### 6.2.1 Ligaments Development

To construct ligaments over the bones, point cloud files of bones were generated in MIMICS to export in CAD software i.e. Solidworks. These point clouds were used to reconstruct the geometry of bones in Solidworks.

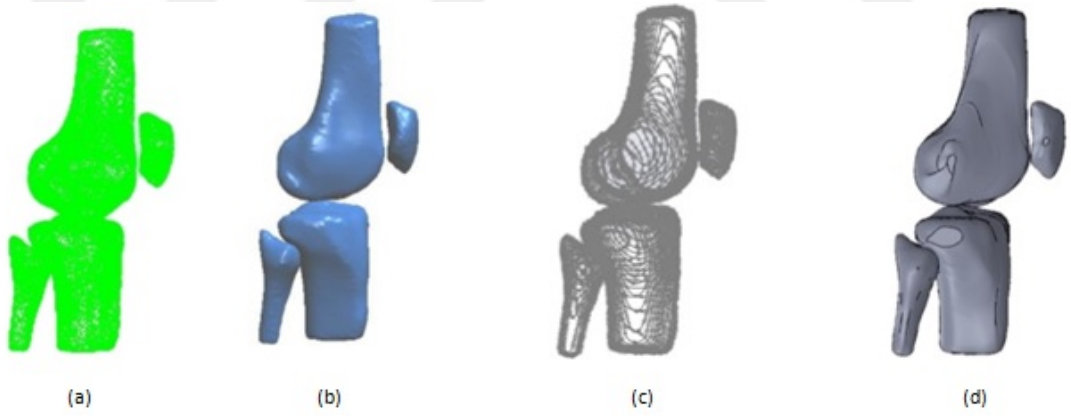


Figure 6.3: a) Point Cloud b) Meshed Point Cloud Surface c) Splines over Surface d) Regenerated Bones

The ligaments were constructed using the loft feature by sketching cross-section of ligaments from where the ligaments are supposed to pass by. The figures below demonstrate the construction of ACL; similar approach was used to create all the ligaments represented as three dimensional structures.


Figure 6.4: a) Sketch of ACL cross-sectional areas b) ACL after loft feature c) ACL in ABAQUS

The slot shaped cross section was selected for representing the ligaments cross sectional area as it closely resembles with the cross section of real ligaments. Furthermore, it is easy to do calculations based on this shape. As the ligaments dimensions are usually given in terms of length-width or cross sectional area. For instance, the cross sectional area of ACL near femoral insertion is 25mm2 and its width and thickness is 13.36mm and 1.75mm respectively. Considering these given dimensions we can the sketch the slot shaped cross section whose area is given by the equation:

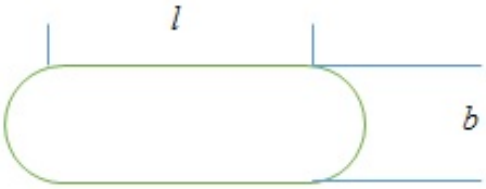


$$A = (l * b) + (\pi * \frac{b^2}{4})$$

Figure 6.5: Calculation of an Area of Slot Shape

Based on the above equation we can change the area, width and thickness parameter in the equation to get the these parameters within the range of published data. Alternatively when only cross-sectional area is given in literature, we can keep the value of area constant and change the thickness and width parameter for sketching the slot shaped cross sectional area. The slot shaped cross

sections are sketched a bit inside the bones so that the loft is extruded inside the bones to avoid any gaps between bone and ligaments insertions. After creating ligaments in Solidworks, they are meshed in IA-FE MESH. Since, ligaments are extruded a bit inside the bones, the elements at the boundary of ligaments are removed in a way that the ligaments boundary closely comply/match with the respective insertion area. The width and thickness of ligaments near insertion area is summarized in the table 1; but SMCL attaches to the bones sideways so its attachment could not be represented by slot shape. Hence, its attachment areas are shown with explained with the figure 6. For ACL,PCL and LCL, their cross-sectional area near insertions was used for coupling them with respective bone. In case of SMCL, its cross sectional area near bony insertions was not used as it attaches sideways to the bones. Hence, its attachment areas are shown with the help of diagram.

Table 6.1: Cross Sectional Area of Ligaments.

| | ACL | | PCL | | LCL | | SMCL | |
|---|---|---|---|---|---|---|---|---|
| | Thickness (mm) | Width (mm) | Thickness (mm) | Width (mm) | Thickness (mm) | Width (mm) | Thickness (mm) | Width (mm) |
| Femur | 1.75 | 13.36 | 3.15 | 11.55 | 4.59 | 9.76 | 3 | 14 |
| Middle Point | 4 | 14 | 3 | 13 | 3 | 12 | 4.59 | 22.4 |
| Tibia | 5.87 | 15.63 | 2.37 | 11.78 | N/A | N/A | 3 | 13 |
| Fibula | N/A | N/A | N/A | N/A | N/A | 8.98 | N/A | N/A |
| Length | 25.38 | | 34.9 | | 48.2 | | 95.8 | |

Note: Above cross sectional areas were used for ligaments attachment on bones for all ligaments except SMCL.

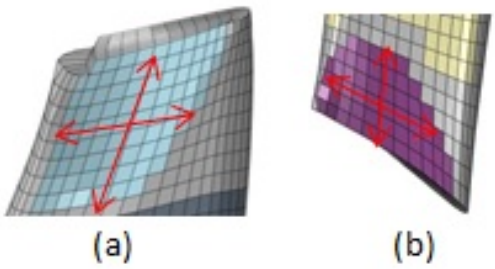


Table 6.2: Areas used for attachment of SMCL, a) on femur; b) on tibia

| | Femur Insertion (mm) | Tibia Insertion (mm) |
|---|---|---|
| Length | 11.6 | 10.5 |
| Width | 7.4 | 10 |

Note:Length is measured along the axis of the bone; width is measure from anterior-posterior plane.

### 6.2.2 Development of Cartilages and Meniscus

The cartilage of femur, tibia and patella was developed by extruding the mesh of the respective bone. The cartilages were extruded based on their thickness obtained from literature [88, 89].

For the development of meniscus, stl files of femoral and tibial cartilage were exported to Solidworks. After reconstructing solid geometry of cartilages in Solidworks, meniscus was made between the cartilages. After several iterations, the final shape of meniscus was obtained which fixed between the femoral and tibial cartilage and was consistent with the dimensions obtained from literature [90–92]. In case of meniscus slot shaped sketch was not used to define meniscal cross sectional areas for passing loft surface. Since the meniscus cross section area is similar to the wedge shape, its cross sectional area was drawn by initially sketching 2 lines representing length and thickness of meniscus. For making the circular perhiperhy of meniscus, the line arc was drawn using endpoints of line representing meniscus thickness. For giving the wedge shaped curvature to the distal meniscus surface, spline was used to sketch it. The spline curve was adjusted based on

the shape of femoral condyles and the line representing length of meniscus was used as a reference to decide the length of spline. Similar approach was used to sketch the proximal wedge shape curvature but in this regards, spline curve was adjusted based on the shape of tibial cartilages. After sketching the proximal and distal curvature of meniscus, the fillet feature was used to make the edges circular of meniscus cross section. The edges of the meniscus cross-section were made circular as the sharp pointy edges lead to severe meshing problems as well as in contact problems in ABAQUS.

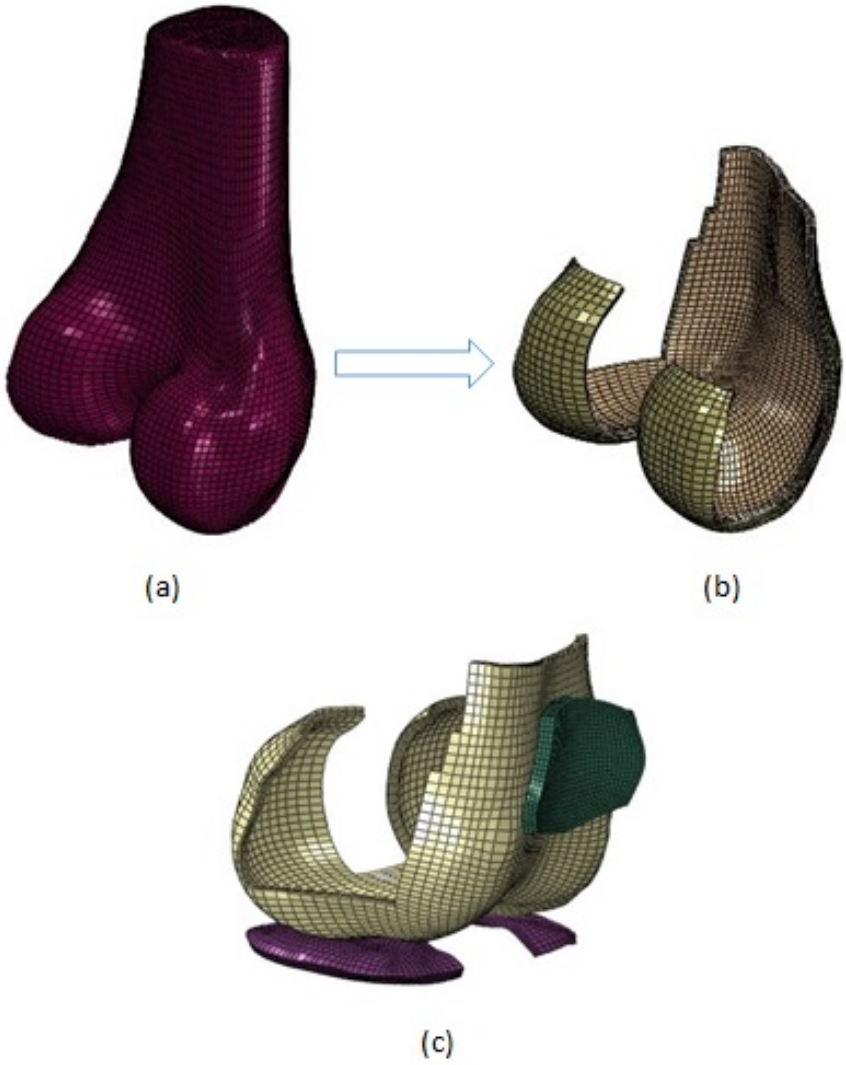


Figure 6.6: a) Femur b) Mesh of femur extruded as a cartilage c) All the cartilages in knee model

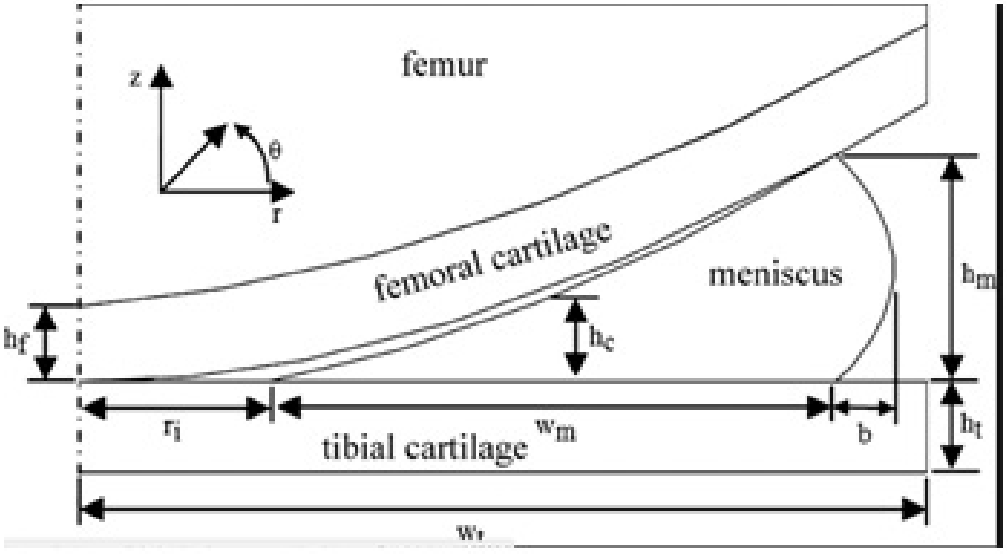


Figure 6.7: Cross section of meniscus [93]


Figure 6.8: a) Cross section of tibial cartilage; b) Sketch of meniscus cross-section

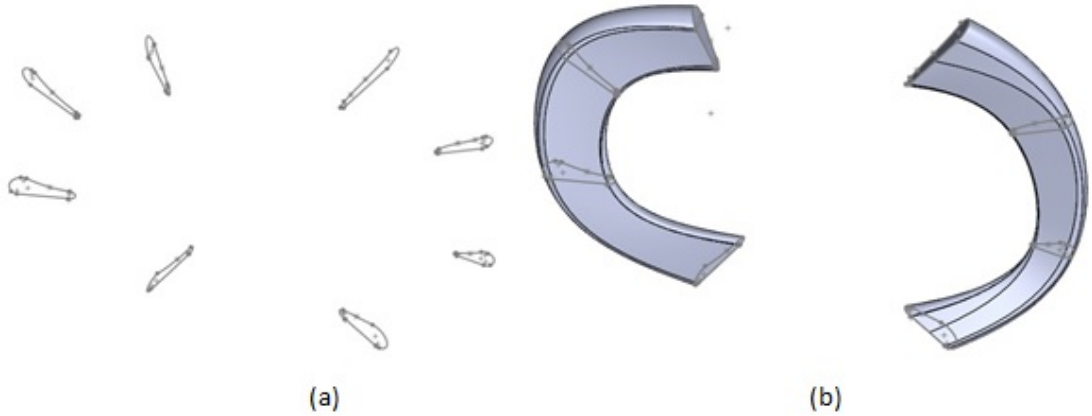


Figure 6.9: a) Sketch for meniscus; b) meniscus

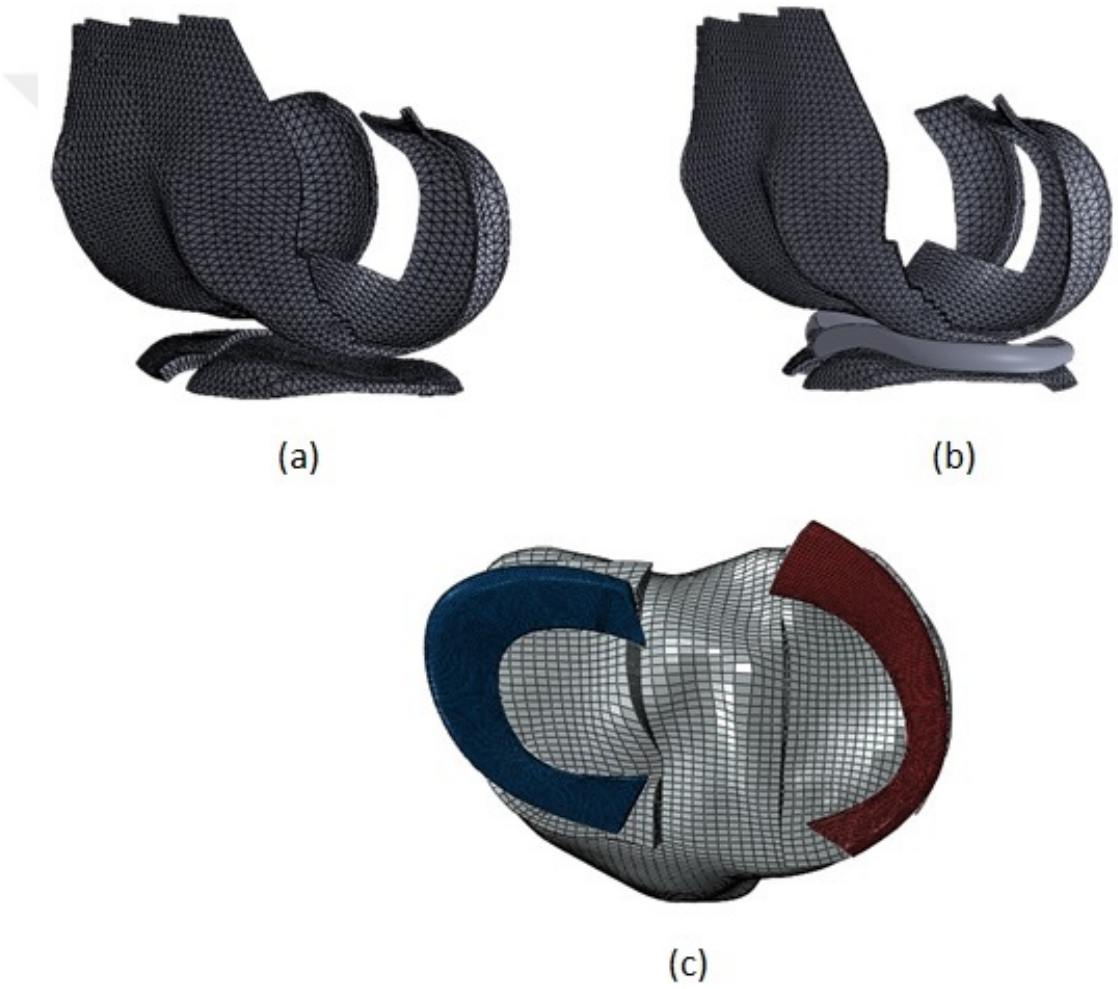


Figure 6.10: a) Surface of cartilages in Solidworks, b) Meniscus created between cartilages, c) top view of meniscus in ABAQUS

## 6.3 Development of Tendons

The patella tendon was developed by the same approach used for ligaments. However, for the application of applying muscle load quadriceps and hamstring tendons were created. Creating these tendons was not easy and required great of amount of time as we only had CT scans of the joint not the whole femur. For that purpose, CT scan of full femur was opted from internet which did not fit with the knee joint but for the sake of proceeding with the model development it was used in the model. Moreover, hamstring tendons have attachments on iliac so the previous FE-model of iliac developed by ORB group was used. To summarize it, we can say that it took 3 different models to get the attachment points of tendons. Once the attachment points were obtained using full femur and iliac, they were excluded from the model and reference points were created in ABAQUS at the points of tendons attachments. Lastly, connector elements were created using those reference points to represent tendons.

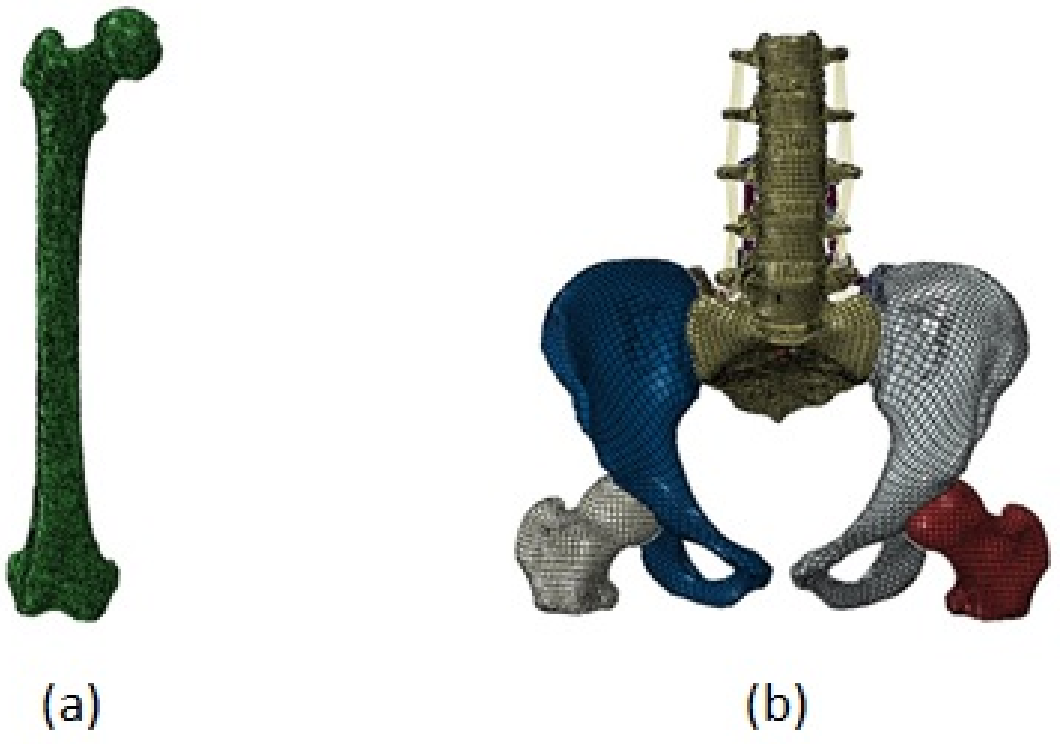

(c)

Figure 6.11: a) Full femur b) Iliac c) Knee joint with tendons

## 6.4 Material Assignment

This section contains the material assignment of all the structures used in the model. Material properties were acquired from the literature. The material properties for hard and soft tissues are summarized in the sub-sections below:

### 6.4.1 Hard Tissues Material

In this study, bones were defined as isotropic linear elastic. Cortical and cancellous layer of bones was taken into consideration and hence their material property was defined using unique properties. The cortical layer properties were different for femur, tibia and patella. The cancellous part of all the bones were given same material property as well as fibula was also defined using cancellous bone property [94, 95].

Table 6.3: Material properties for bones

| **Femur Cortical** | | | **Patella Cortical** | |
|---|---|---|---|---|
| Young's Modulus (Mpa) | Poisson's Ratio | Shear Modulus (Mpa) | Young's Modulus (Mpa) | Poisson's Ratio |
| E1 = 12000 | 12 = 0.38 | G12 = 4347 | E = 15000 | = 0.3 |
| E2 = 13400 | 13 = 0.22 | G13 = 5492 | **Cancellous Bone** | |
| E3 = 20000 | 23 = 0.24 | G23 = 8065 | Young's Modulus (Mpa) | Poisson's Ratio |
| **Tibia Cortical** | | | E = 400 | = 0.3 |
| Young's Modulus (Mpa) | Poisson's Ratio | Shear Modulus (Mpa) | | |
| E1 = 6900 | 12 = 0.49 | G12 = 2315 | | |
| E2 = 8500 | 13 = 0.12 | G13 = 3795 | | |
| E3 = 18400 | 23 = 0.14 | G23 = 8070 | | |

Note: Direction 1 is radial, 2 is circumferential and 3 is axial (along the axis of the bone)

### 6.4.2 Soft Tissues Property

The cruciate (Anterior Cruciate Ligament/Posterior Cruciate Ligament) and collateral ligaments (Medial Collateral Ligament/Lateral Collateral Ligament) were

represented using hyper-elastic isotropic material. The stress-strain data for collateral ligaments and patella tendon was given as an input to ABAQUS using hyperelastic Ogden formulization with SED of 1 [96, 97].

Table 6.4: Stress-Strain Data for MCL/LCL/Patella Tendon

| **MCL/LCL** | | **Patella Tendon** | |
|---|---|---|---|
| Stress(Mpa) | Strain(%) | Stress(Mpa) | Strain(%) |
| 1.61 | 0.02 | 2.9 | 0.01 |
| 5.51 | 0.042 | 7.1 | 0.02 |
| 6.69 | 0.048 | 16.1 | 0.037 |
| 8.14 | 0.054 | 23.3 | 0.048 |
| 9.49 | 0.06 | 34.9 | 0.066 |
| 10.93 | 0.066 | 50.6 | 0.096 |
| 12.54 | 0.072 | 52.4 | 0.099 |
| 14.15 | 0.078 | 57.6 | 0.109 |
| 15.72 | 0.084 | 68.3 | 0.135 |
| 17.25 | 0.09 | | |
| 18.81 | 0.096 | | |
| 20.25 | 0.102 | | |
| 21.86 | 0.108 | | |
| 22.46 | 0.111 | | |

For cruciate ligaments, stress-strain data was given as an input to ABAQUS but SED of 2 was used as reported in literature [87, 98]. However, using SED of 2 was leading to material instability while using test data as an input to ABAQUS and selecting SED of 2. So, in order to progress with model validation material constants for Ogden model were obtained manually by trial and error method. The constants were manually adjusted until the stress-stain curve obtained from literature them closely resembled with the curve obtained from literature [**?**].

Table 6.5: Stress-Strain Data for ACL and PCL

| **ACL** | | **PCL** | |
|---|---|---|---|
| Stress(Mpa) | Strain(%) | Stress(Mpa) | Strain(%) |
| 1.44 | 0.01 | 1.05 | 0.01 |
| 3.34 | 0.02 | 2.69 | 0.02 |
| 5.7 | 0.03 | 4.79 | 0.03 |
| 8.85 | 0.04 | 7.21 | 0.04 |
| 13.11 | 0.05 | 10.23 | 0.05 |
| 17.25 | 0.06 | 13.51 | 0.06 |
| 21.25 | 0.07 | 17.25 | 0.07 |
| 25.44 | 0.08 | 20.46 | 0.08 |
| 29.84 | 0.09 | 24.26 | 0.09 |
| 33.51 | 0.1 | 27.74 | 0.1 |
| 36.66 | 0.11 | 31.41 | 0.11 |
| 39.08 | 0.12 | 34.82 | 0.12 |

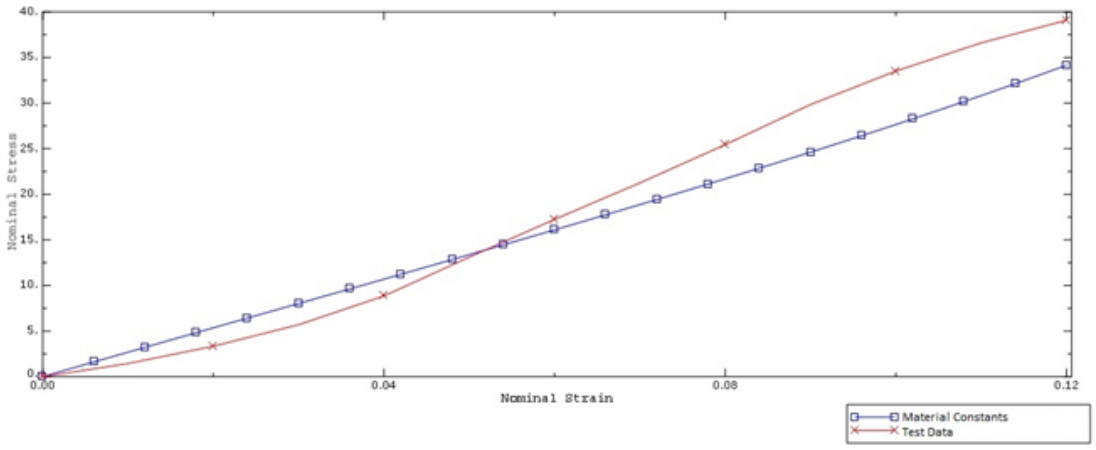


Figure 6.12: Curve fit for ACL

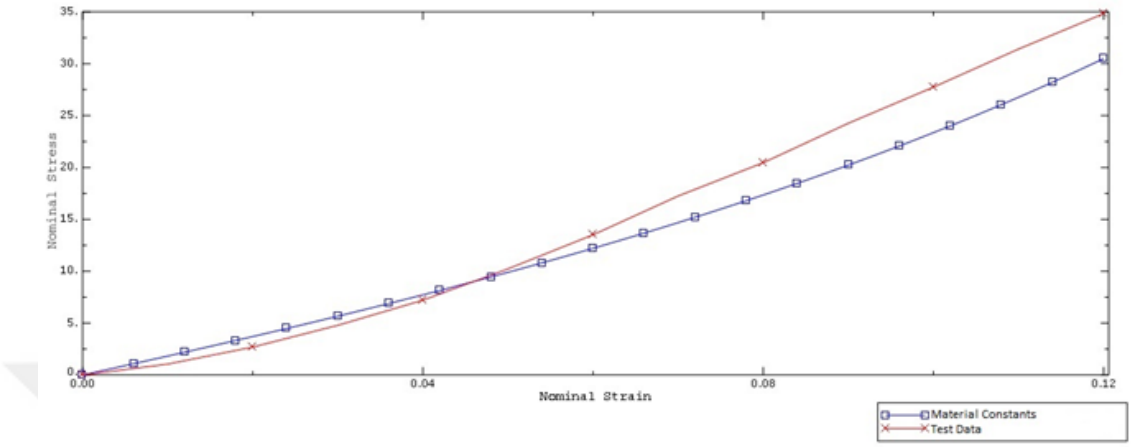


Figure 6.13: Curve fit for PCL

Table 6.6: Ogden model material constants for ACL and PCL

| | **mu1** | **alpha1** | **mu2** | **alpha2** | **D1** | **D2** |
|---|---|---|---|---|---|---|
| **ACL** | 80 | 2 | 10 | 20 | 0 | 0 |
| **PCL** | 20 | 2 | 40 | 15 | 0 | 0 |

The material property for ligaments represented using truss elements was obtained in terms of stiffness but in the model stiffness values are used as young modulus with a poissons ratio assumed to be 0.45 as most soft tissues have poissons ratio near to this value. The meniscus was defined using transversely isotropic material having different material property in axial, circumferential and radial direction.

Table 6.7: Material property for meniscus

| **Meniscus** | |
|---|---|
| Young's Modulus (Mpa) | Poisson's Ratio |
| E1 = 20 | 12 = 0.3 |
| E2 = 120 | 13 = 0.45 |
| E3 = 20 | 23 = 0.3 |

Note: Direction 1 is radial, 2 is circumferential and 3 is axial

Table 6.8: Material property for ligaments represented by truss elements

| **Ligaments Represented by Truss Elements** | |
|---|---|
| | Stiffness (N/mm) |
| Post.Capsule Lateral (CAPl) | 54.6 |
| Post.Capsule Medial (CAPm) | 52.6 |
| Post.Capsule Oblique (CAPo) | 21.4 |
| Post.Capsule Arcuate (CAPa) | 20.8 |
| Medial Patellofemoral Ligament (MPFL) | 16 |
| Lateral Patellofemoral Ligament (LPFL) | 12 |

## 6.5 Couplings and Interactions

The ligaments were attached to the bones using coupling constraint in ABAQUS, for meniscus the lower surface of meniscus was coupled with the tibial cartilage. For defining the interactions, surface to surface frictionless contact formulization was used. The interactions were defined between femoral cartilage-tibial cartilage, femoral cartilage-patellar cartilage, femoral cartilage-meniscus, MCL-tibia, MCL-femur, ACL-PCL.

## 6.6 Model Validation

This section discusses the boundary conditions, interactions and loading protocols used for model validation. The loading protocols for validating the model were opted from literature and similar loadings were applied in our knee model.

### 6.6.1 Tibiofemoral Kinematics Validation

Two sets of loading protocols were used to validate the tibiofemoral kinematics and the boundary conditions were applied accordingly. Before applying any load, initial displacement of 0.8mm was given to tibia to establish the contact between femur and tibia then muscle load of 400N and 200N is applied through quadriceps

and hamstring tendons respectively. Later, during the first loading protocol, femur is fixed and valgus moment is applied from (0-50Nm) with tibia fixed at 25 degrees flexion. In the second loading protocol, femur is fixed at full extension and tibia is flexed between (0-50) degrees with an interval of 5 degrees than 15Nm internal moment is applied to tibia at every interval [87].

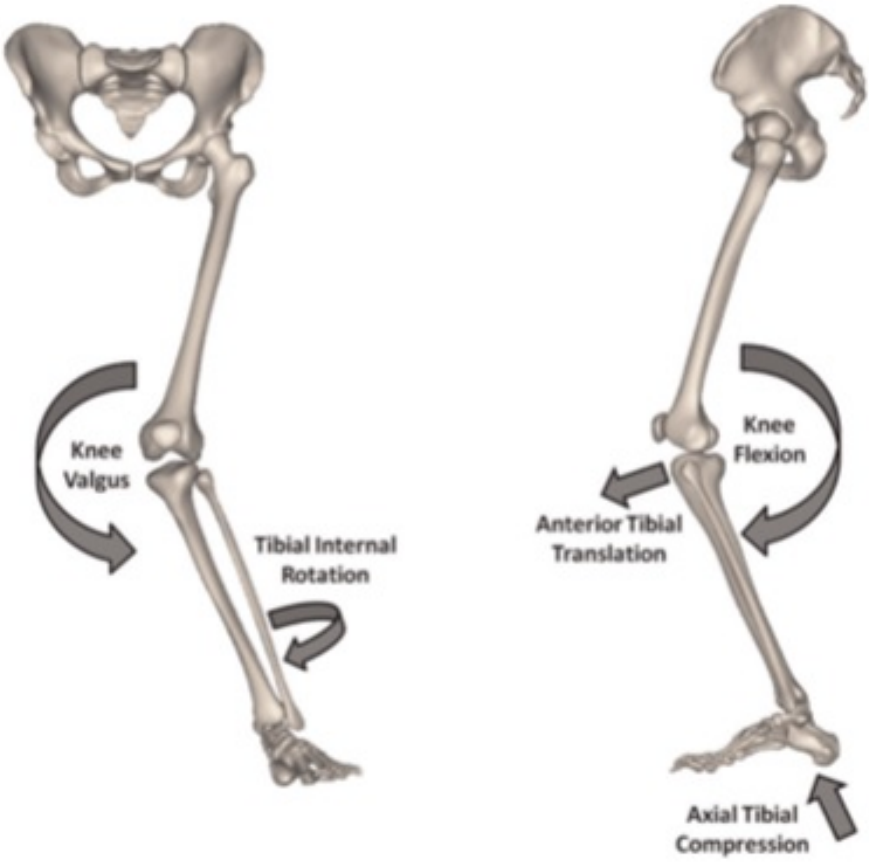


Figure 6.14: Knee joint loading conventions [87]

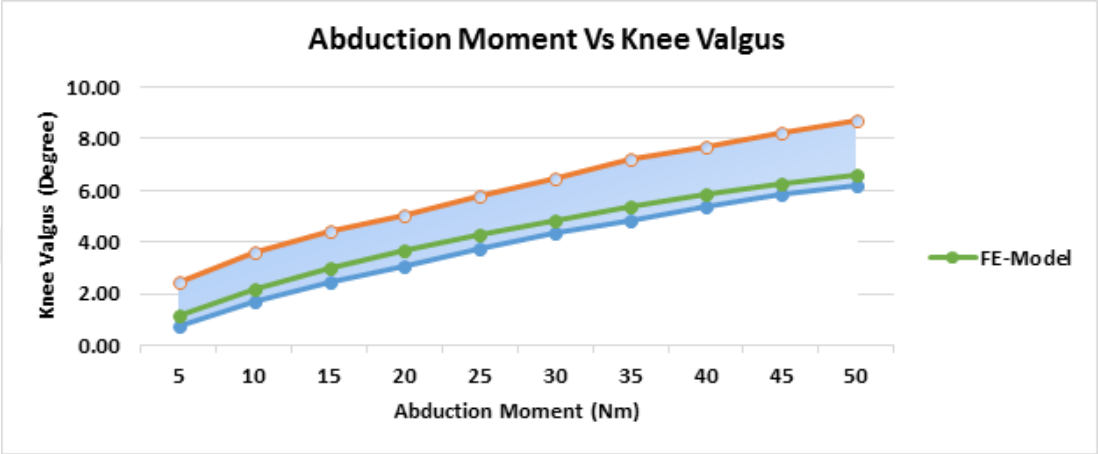


Figure 6.15: FE predictions vs experimental data for knee valgus while tibia is fixed at 25deg flexion

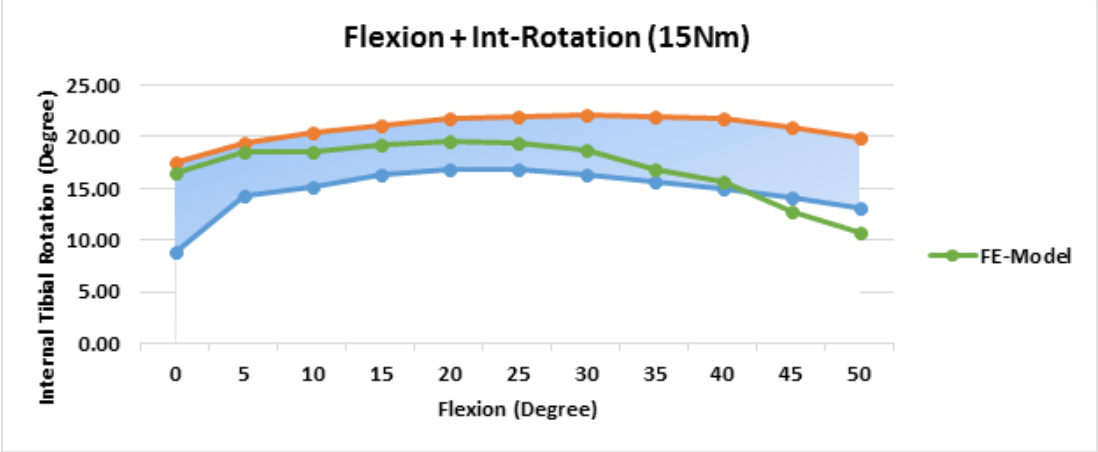


Figure 6.16: FE predictions vs experimental data for internal tibial rotation

### 6.6.2 Patellofemoral Kinematics Validation

The boundary conditions for patellofemoral validation were changed based on the loading protocol. Before applying any load, initial displacement of 0.8mm was given to femur to establish the contact between femur and tibia. Then, tibia is constrained in all degrees of freedom and femur is flexed from (0-50) degrees under the 200N quadriceps load [99].

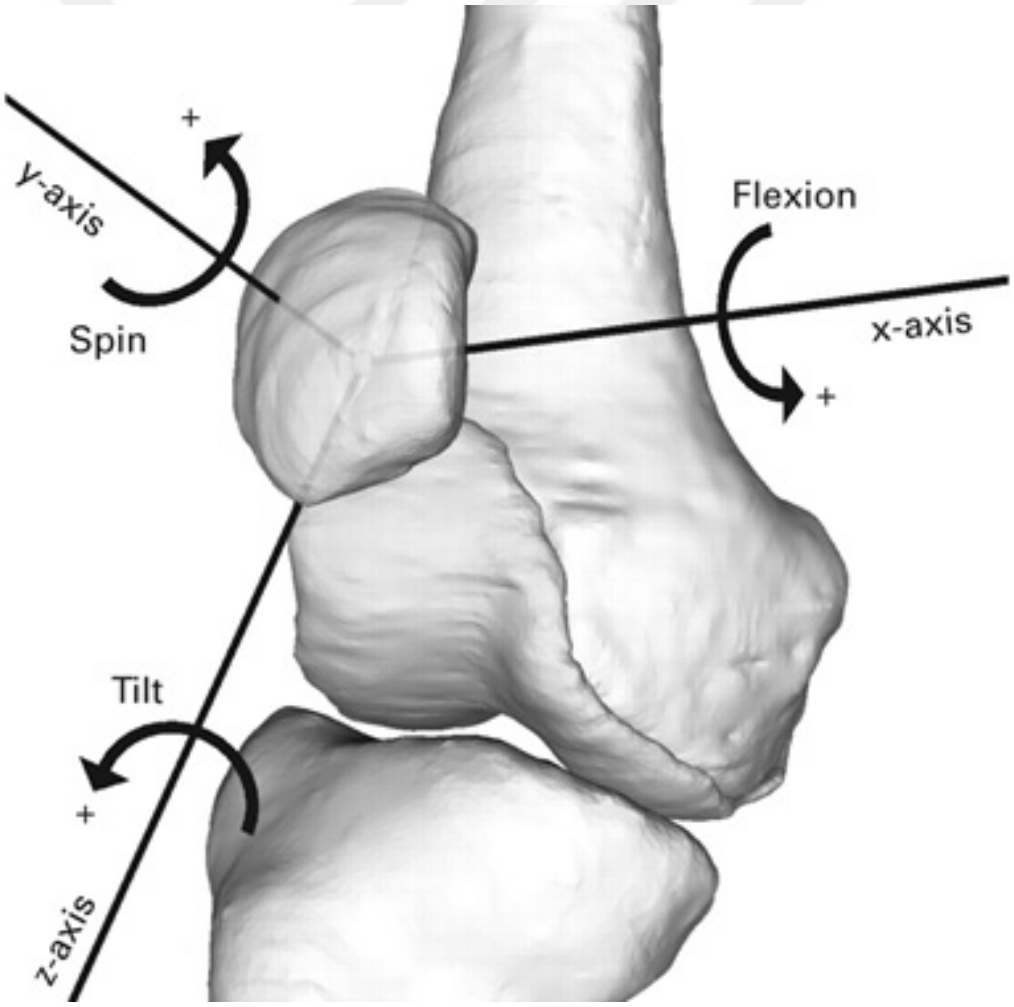


Figure 6.17: Analogy of patellar kinematics
Image Courtesy:http://www.bjj.boneandjoint.org.uk/content/89-B/6/752)

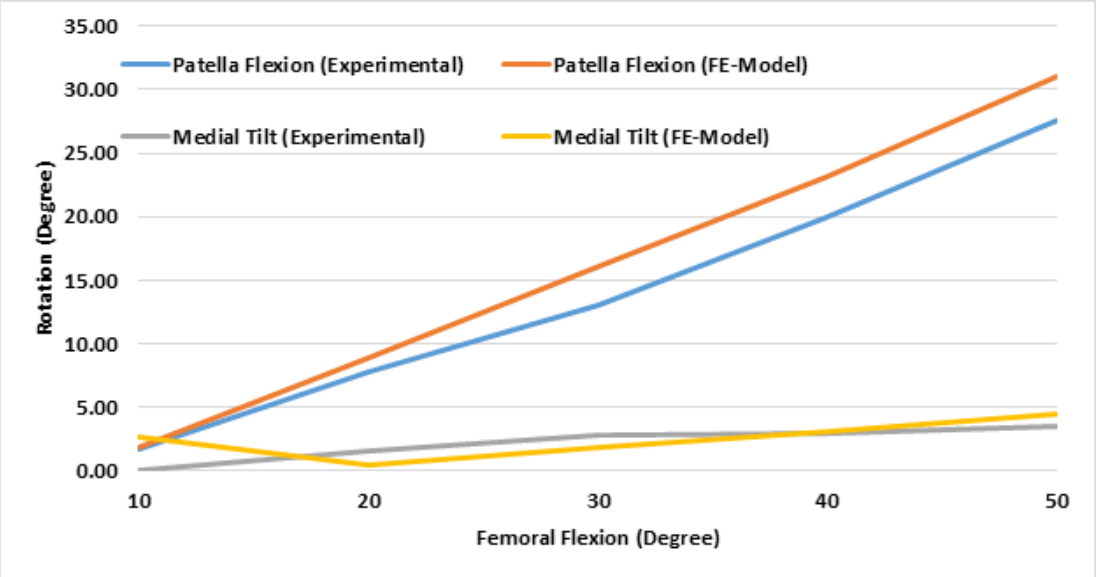


Figure 6.18: FE-predictions vs experimental data for patellofemoral kinematics

## 6.7 Conclusion

The results obtained for knee joint kinematics are in close approximation with the literature. The validation of the model can be increased by comparing it with other studies but for that the model has to be made more accurate. Since the CT scans used in this study, were not specifically opted for the purpose of model development, it was observed that the distance between femur and tibia is very small. It can be due to various reasons such as CT scans must have been taken in a position where the joint is under some compressive load or so. Other reason could be that, the extreme layer of femur and tibia is actually cartilage but due to lack of experience in interpreting CT scans we are unable to distinguish between bone and cartilage. Moreover, it is also possible that the individuals cartilage and meniscus are thin as compared to a normal persons cartilage. To overcome the issue of small cavity between tibia and femur, it was not possible to fit the cartilages and meniscus in that cavity. Therefore, the gap between femur and tibia was increased. This gap was adjusted iteratively by fitting in cartilages and meniscus of different thickness opted from literature [88–92]. The CT scans used in this study were of the knee joint only. In order to apply muscle loads, model of full femur was taken from the internet and the iliac was added from the ORB

groups previous model. Assembling these models together for identifying muscles attachments would have obviously added an error in our model. The muscles attachment points can be identified more accurately if the entire data belongs to one individual.

# Bibliography


[1] M. Bhatnagar, P. D. Sponseller, C. Carroll IV, and V. T. Tolo, "Pediatric atlantoaxial instability presenting as cerebral and cerebellar infarcts.," *Journal of Pediatric Orthopaedics*, vol. 11, no. 1, pp. 103–107, 1991.

[2] W. A. Bonadio, "Cervical spine trauma in children: Part i. general concepts, normal anatomy, radiographic evaluation," *The American journal of emergency medicine*, vol. 11, no. 2, pp. 158–165, 1993.

[3] W. A. Bonadio, "Cervical spine trauma in children: Part ii. mechanisms and manifestations of injury, therapeutic considerations," *The American journal of emergency medicine*, vol. 11, no. 3, pp. 256–278, 1993.

[4] J. Godersky and A. Menezes, "Optimal management for children with spinal cord injury," *Contemp Neurosurg*, vol. 11, no. 1, pp. 1–6, 1989.

[5] A. H. Menezes and V. C. Traynelis, "Anatomy and biomechanics of normal craniovertebral junction (a) and biomechanics of stabilization (b)," *Child's Nervous System*, vol. 24, no. 10, pp. 1091–1100, 2008.

[6] N. Bogduk and S. Mercer, "Biomechanics of the cervical spine. i: Normal kinematics," *Clinical biomechanics*, vol. 15, no. 9, pp. 633–648, 2000.

[7] J. Dvorak, E. Schneider, P. Saldinger, and B. Rahn, "Biomechanics of the craniocervical region: the alar and transverse ligaments," *Journal of Orthopaedic Research*, vol. 6, no. 3, pp. 452–461, 1988.

[8] A. M. Robert and R. Jr. Ashraf A, "Occipitocervical region." http://neupsykey.com/occipitocervical-region/. Aug, 2016.

[9] F. Schwab, V. Lafage, R. Boyce, W. Skalli, and J.-P. Farcy, "Gravity line analysis in adult volunteers: age-related correlation with spinal parameters, pelvic parameters, and foot position," *Spine*, vol. 31, no. 25, pp. E959–E967, 2006.

[10] V. Lafage, F. Schwab, W. Skalli, N. Hawkinson, P.-M. Gagey, S. Ondra, and J.-P. Farcy, "Standing balance and sagittal plane spinal deformity: analysis of spinopelvic and gravity line parameters," *Spine*, vol. 33, no. 14, pp. 1572–1578, 2008.

[11] D. Steilen, R. Hauser, B. Woldin, and S. Sawyer, "Chronic neck pain: making the connection between capsular ligament laxity and cervical instability," *The open orthopaedics journal*, vol. 8, p. 326, 2014.

[12] "Atlas of anatomy." http://doctorlib.info/medical/anatomy/3.html. n.d.

[13] H. M. Team, "Bodymaps." http://www.healthline.com/human-body-maps/femur. April, 2015.

[14] B. Anatomy, "Femur." http://benfisheranatomy.weebly.com/femur.html. n.d.

[15] J. Oliver, "The tibia." http://teachmeanatomy.info/lower-limb/bones/the-tibia/. January, 2017.

[16] Boundless, "Tibia and fibula (the leg)." http://www.boundless.com/physiology/textbooks/boundless-anatomy-and-physiology-textbook/skeletal-system-parts-of-the-skeleton-7/the-lower-limb-88/tibia-and-fibula-the-leg-497-4321/. n.d.

[17] H. Dr. Craig and et al, "Tibia." https://radiopaedia.org/articles/tibia. n.d.

[18] Boundless, "Patella (the knee)," n.d.

[19] "The patella." http://anatomy-medicine.com/musculoskeletal-system/79-the-patella.html. n.d.

[20] J. A. Koski, C. Ibarra, S. A. Rodeo, and R. F. Warren, "Meniscal injury and repair: clinical status," *Orthopedic Clinics of North America*, vol. 31, no. 3, pp. 419–435, 2000.

[21] "Meniscus function." http://www.ivysportsmed.com/en/knee-pain/meniscus-function. n.d.

[22] P. Bryn Mawr, "Articular cartilage." www50.safesecureweb.com/secure/. July,2012.

[23] "Ligaments of the knee." http://www.newhealthadvisor.com/Ligaments-of-the-Knee.html. June,2017.

[24] D. Rick Wilkerson and M. Stuart J. Fischer, "Patellar tendon tear." http://orthoinfo.aaos.org/topic.cfm?topic=a00512. February, 2016.

[25] "Hamstring muscle injuries." http://orthoinfo.aaos.org/topic.cfm?topic=a00408. July, 2015.

[26] W. Gallie, "Fractures and dislocations of the cervical spine," *The American Journal of Surgery*, vol. 46, no. 3, pp. 495–499, 1939.

[27] M. D. Smith, W. A. Phillips, and R. N. Hensinger, "Complications of fusion to the upper cervical spine.," *Spine*, vol. 16, no. 7, pp. 702–705, 1991.

[28] D. Grob, J. J. Crisco III, M. M. Panjabi, P. Wang, and J. Dvorak, "Biomechanical evaluation of four different posterior atlantoaxial fixation techniques.," *Spine*, vol. 17, no. 5, pp. 480–490, 1992.

[29] G. K. Geremia, K. S. Kim, L. Cerullo, and L. Calenoff, "Complications of sublaminar wiring," *Surgical neurology*, vol. 23, no. 6, pp. 629–634, 1985.

[30] S. L. Huhn, A. L. Wolf, and J. Ecklund, "Technical note: Posterior spinal osteosynthesis for cervical fracture/dislocation using a flexible multistrand cable system: Technical note.," *Neurosurgery*, vol. 29, no. 6, pp. 943–946, 1991.

[31] M. N. Songer, D. L. Spencer, P. R. Meyer, and G. Jayaraman, "The use of sublaminar cables to replace luque wires.," *Spine*, vol. 16, no. 8, p. S422, 1991.

[32] J. Harms and R. P. Melcher, "Posterior c1–c2 fusion with polyaxial screw and rod fixation," *Spine*, vol. 26, no. 22, pp. 2467–2471, 2001.

[33] A. Goel and V. Laheri, "Plate and screw fixation for atlanto-axial subluxation," *Acta neurochirurgica*, vol. 129, no. 1, pp. 47–53, 1994.

[34] D.-G. Huang, D.-J. Hao, B.-R. He, Q.-N. Wu, T.-J. Liu, X.-D. Wang, H. Guo, and X.-Y. Fang, "Posterior atlantoaxial fixation: a review of all techniques," *The Spine Journal*, vol. 15, no. 10, pp. 2271–2281, 2015.

[35] B. Jeanneret and F. Magerl, "Primary posterior fusion c1/2 in odontoid fractures: indications, technique, and results of transarticular screw fixation.," *Clinical Spine Surgery*, vol. 5, no. 4, pp. 464–475, 1992.

[36] N. M. Wright, "Posterior c2 fixation using bilateral, crossing c2 laminar screws: case series and technical note," *Clinical Spine Surgery*, vol. 17, no. 2, pp. 158–162, 2004.

[37] W. Jean-Paul and R. Yassari, "Atlantoaxial instability and stabilization." https://clinicalgate.com/atlantoaxial-instability-and-stabilization/. March,2015.

[38] OrthoConsult, "Magerl screws (c1-c2 transarticular screw)." http://www.orthoconsult.com/magerl-screws-c1-c2-transarticular-screw/. May,2015.

[39] J. Harms and R. P. Melcher, "Posterior c1–c2 fusion with polyaxial screw and rod fixation," *Spine*, vol. 26, no. 22, pp. 2467–2471, 2001.

[40] F. Kandziora, R. Pflugmacher, J. Schaefer, M. Scholz, K. Ludwig, P. Schleicher, and N. P. Haas, "Biomechanical comparison of expandable cages for vertebral body replacement in the cervical spine," *Journal of Neurosurgery: Spine*, vol. 99, no. 1, pp. 91–97, 2003.

[41] C. Brenke, S. Fischer, A. Carolus, K. Schmieder, and G. Ening, "Complications associated with cervical vertebral body replacement with expandable titanium cages," *Journal of Clinical Neuroscience*, vol. 32, pp. 35–40, 2016.

[42] S. Hartmann, C. Thomé, A. Tschugg, J. Paesold, P. Kavakebi, and W. Schmölz, "Cement-augmented screws in a cervical two-level corpectomy with anterior titanium mesh cage reconstruction: a biomechanical study," *European Spine Journal*, vol. 26, no. 4, pp. 1047–1057, 2017.

[43] Z. Li, Y. Zhao, J. Tang, D. Ren, J. Guo, H. Wang, L. Li, and S. Hou, "A comparison of a new zero-profile, stand-alone fidji cervical cage and anterior cervical plate for single and multilevel acdf: a minimum 2-year follow-up study," *European Spine Journal*, vol. 26, no. 4, pp. 1129–1139, 2017.

[44] R. J. Hacker, J. C. Cauthen, T. J. Gilbert, and S. L. Griffith, "A prospective randomized multicenter clinical evaluation of an anterior cervical fusion cage," *Spine*, vol. 25, no. 20, pp. 2646–2655, 2000.

[45] L. Hattou, X. Morandi, J. Lefebvre, P.-J. Le Reste, L. Riffaud, and P.-L. Hénaux, "Anterior cervical interbody fusion using polyetheretherketone cage filled with synthetic bone graft in acute cervical spine injury," *Orthopaedics & Traumatology: Surgery & Research*, vol. 103, no. 1, pp. 61–66, 2017.

[46] Z.-j. Li, Y. Wang, G.-j. Xu, and P. Tian, "Is peek cage better than titanium cage in anterior cervical discectomy and fusion surgery? a meta-analysis," *BMC musculoskeletal disorders*, vol. 17, no. 1, p. 379, 2016.

[47] P. X. Montesano, E. C. Juach, P. A. Anderson, D. R. Benson, and P. B. Hanson, "Biomechanics of cervical spine internal fixation.," *Spine*, vol. 16, no. 3, pp. S10–S16, 1991.

[48] S. H. Kim, D. A. Shin, S. Yi, D. H. Yoon, K. N. Kim, and H. C. Shin, "Early results from posterior cervical fusion with a screw-rod system," *Yonsei medical journal*, vol. 48, no. 3, pp. 440–448, 2007.

[49] J. K. Lee, S. K. Jung, Y.-S. Lee, S. R. Jeon, S. W. Roh, S. C. Rhim, and J. H. Park, "Analysis of the fusion and graft resorption rates, as measured by

computed tomography, 1 year after posterior cervical fusion using a cervical pedicle screw," *World Neurosurgery*, vol. 99, pp. 171–178, 2017.

[50] T. L. Johnston, E. E. Karaikovic, E. P. Lautenschlager, and D. Marcu, "Cervical pedicle screws vs. lateral mass screws: uniplanar fatigue analysis and residual pullout strengths," *The Spine Journal*, vol. 6, no. 6, pp. 667–672, 2006.

[51] L. Ronald, R. Daniel, and S. Klaus, "Occipitocervical fusion (screw fixation)." https://www2.aofoundation.org/. n.d.

[52] Zimmer, "Spine, pathfinder nxt minimally invasive pedicle screw system.." http://www.zimmer-finland.com/fi-FI/hcp/spine/product/pathfinder-minimally-invasive-pedicle-screw.jspx. n.d.

[53] P. Schleicher, M. Scholz, A. Pingel, and F. Kandziora, "Traumatic spondylolisthesis of the axis vertebra in adults," *Global spine journal*, vol. 5, no. 04, pp. 346–358, 2015.

[54] D. Coric, P. K. Kim, J. D. Clemente, M. O. Boltes, M. Nussbaum, and S. James, "Prospective randomized study of cervical arthroplasty and anterior cervical discectomy and fusion with long-term follow-up: results in 74 patients from a single site: clinical article," *Journal of Neurosurgery: Spine*, vol. 18, no. 1, pp. 36–42, 2013.

[55] J. Dejaegher, J. Walraevens, J. van Loon, F. Van Calenbergh, P. Demaerel, and J. Goffin, "10-year follow-up after implantation of the bryan cervical disc prosthesis," *European Spine Journal*, vol. 26, no. 4, pp. 1191–1198, 2017.

[56] A. A. Gandhi, "Biomechanical analysis of the cervical spine following total disc arthroplasty: an experimental and finite element investigation," 2012.

[57] R. C. Sasso, N. H. Metcalf, J. A. Hipp, N. D. Wharton, and P. A. Anderson, "Sagittal alignment after bryan cervical arthroplasty," *Spine*, vol. 36, no. 13, pp. 991–996, 2011.

[58] S. W. Kim, J. H. Shin, J. J. Arbatin, M. S. Park, Y. K. Chung, and P. C. McAfee, "Effects of a cervical disc prosthesis on maintaining sagittal alignment of the functional spinal unit and overall sagittal balance of the cervical spine," *European Spine Journal*, vol. 17, no. 1, pp. 20–29, 2008.

[59] T. P. Loumeau, B. V. Darden, T. J. Kesman, S. M. Odum, B. A. Van Doren, E. B. Laxer, and D. B. Murrey, "A rct comparing 7-year clinical outcomes of one level symptomatic cervical disc disease (scdd) following prodisc-c total disc arthroplasty (tda) versus anterior cervical discectomy and fusion (acdf)," *European Spine Journal*, vol. 25, no. 7, pp. 2263–2270, 2016.

[60] D. J. Diangelo, K. T. Foley, B. R. Morrow, J. S. Schwab, J. Song, J. W. German, and E. Blair, "In vitro biomechanics of cervical disc arthroplasty with the prodisc-c total disc implant," *Neurosurgical focus*, vol. 17, no. 3, pp. 44–54, 2004.

[61] J. K. Burkus, V. C. Traynelis, R. W. Haid Jr, and P. V. Mummaneni, "Clinical and radiographic analysis of an artificial cervical disc: 7-year follow-up from the prestige prospective randomized controlled clinical trial: Clinical article," *Journal of Neurosurgery: Spine*, vol. 21, no. 4, pp. 516–528, 2014.

[62] P. V. Mummaneni, J. K. Burkus, R. W. Haid, V. C. Traynelis, and T. A. Zdeblick, "Clinical and radiographic analysis of cervical disc arthroplasty compared with allograft fusion: a randomized controlled clinical trial," *Journal of Neurosurgery: Spine*, vol. 6, no. 3, pp. 198–209, 2007.

[63] J. K. Burkus, R. W. Haid Jr, V. C. Traynelis, and P. V. Mummaneni, "Long-term clinical and radiographic outcomes of cervical disc replacement with the prestige disc: results from a prospective randomized controlled clinical trial: Clinical article," *Journal of Neurosurgery: Spine*, vol. 13, no. 3, pp. 308–318, 2010.

[64] A. Vaccaro, W. Beutler, W. Peppelman, J. M. Marzluff, J. Highsmith, A. Mugglin, G. DeMuth, M. Gudipally, and K. J. Baker, "Clinical outcomes with selectively constrained secure-c cervical disc arthroplasty: two-year results from a prospective, randomized, controlled, multicenter investigational device exemption study," *Spine*, vol. 38, no. 26, pp. 2227–2239, 2013.

[65] M. S. Hisey, H. W. Bae, R. J. Davis, S. Gaede, G. Hoffman, K. D. Kim, P. D. Nunley, D. Peterson, R. F. Rashbaum, J. Stokes, *et al.*, "Prospective, randomized comparison of cervical total disk replacement versus anterior cervical fusion: results at 48 months follow-up," *Clinical Spine Surgery*, vol. 28, no. 4, pp. E237–E243, 2015.

[66] F. M. Phillips, J. Y. Lee, F. H. Geisler, A. Cappuccino, C. D. Chaput, J. G. DeVine, C. Reah, K. M. Gilder, K. M. Howell, and P. C. McAfee, "A prospective, randomized, controlled clinical investigation comparing pcm cervical disc arthroplasty with anterior cervical discectomy and fusion: 2-year results from the us fda ide clinical trial," *Spine*, vol. 38, no. 15, pp. E907–E918, 2013.

[67] LDR, "Mobi-c cervical disc." https://us.ldr.com/Products/Cervical/MobiC n.d.

[68] K. Brolin and P. Halldin, "Development of a finite element model of the upper cervical spine and a parameter study of ligament characteristics," *Spine*, vol. 29, no. 4, pp. 376–385, 2004.

[69] M. Panjabi, J. Dvorak, J. Crisco III, *et al.*, "Flexion, extension, and lateral bending of the upper cervical spine in response to alar ligament transections.," *Clinical Spine Surgery*, vol. 4, no. 2, pp. 157–167, 1991.

[70] M. Panjabi, J. Dvorak, J. J. Crisco, T. Oda, P. Wang, and D. Grob, "Effects of alar ligament transection on upper cervical spine rotation," *Journal of orthopaedic research*, vol. 9, no. 4, pp. 584–593, 1991.

[71] M. Panjabi, J. Dvorak, J. J. Crisco, T. Oda, P. Wang, and D. Grob, "Cervical spine protection report," *Prepared for NOCSAE*, vol. 30, 1995.

[72] I. G. Dorward and N. M. Wright, "Seven years of experience with c2 translaminar screw fixation: clinical series and review of the literature," *Neurosurgery*, vol. 68, no. 6, pp. 1491–1499, 2011.

[73] R. A. Lehman, A. E. Dmitriev, and K. W. Wilson, "Biomechanical analysis of the c2 intralaminar fixation technique using a cross-link and offset connector

for an unstable atlantoaxial joint," *The Spine Journal*, vol. 12, no. 2, pp. 151–156, 2012.

[74] S. B. Lapsiwala, P. A. Anderson, A. Oza, and D. K. Resnick, "Biomechanical comparison of four c1 to c2 rigid fixative techniques: anterior transarticular, posterior transarticular, c1 to c2 pedicle, and c1 to c2 intralaminar screws," *Neurosurgery*, vol. 58, no. 3, pp. 516–521, 2006.

[75] J. Gorek, E. Acaroglu, S. Berven, A. Yousef, and C. M. Puttlitz, "Constructs incorporating intralaminar c2 screws provide rigid stability for atlantoaxial fixation," *Spine*, vol. 30, no. 13, pp. 1513–1518, 2005.

[76] D. Erbulut, I. Zafarparandeh, I. Lazoglu, and A. Ozer, "Application of an asymmetric finite element model of the c2-t1 cervical spine for evaluating the role of soft tissues in stability," *Medical engineering & physics*, vol. 36, no. 7, pp. 915–921, 2014.

[77] G. R. Fogel, G. Zhang, and P. Weiqiang Liu, "Biomechanical analysis of two-level cervical disc replacement with a stand-alone u-shaped disc implant," 2017.

[78] Z. J. Mo, Y. B. Zhao, L. Z. Wang, Y. Sun, M. Zhang, and Y. B. Fan, "Biomechanical effects of cervical arthroplasty with u-shaped disc implant on segmental range of motion and loading of surrounding soft tissue," *European spine journal*, vol. 23, no. 3, pp. 613–621, 2014.

[79] M. Eldin and M. Mohamed, "Dynamic cervical implant (dci) in single level cervical disc disease," *The Open Spine Journal*, vol. 6, no. 1, 2014.

[80] A. Amis, C. Gupte, A. Bull, and A. Edwards, "Anatomy of the posterior cruciate ligament and the meniscofemoral ligaments," *Knee Surgery, Sports Traumatology, Arthroscopy*, vol. 14, no. 3, pp. 257–263, 2006.

[81] J.-M. Brinkman, P. Schwering, L. Blankevoort, J. Koolos, J. Luites, and A. Wymenga, "The insertion geometry of the posterolateral corner of the knee," *Bone & Joint Journal*, vol. 87, no. 10, pp. 1364–1368, 2005.

[82] S. Kopf, V. Musahl, S. Tashman, M. Szczodry, W. Shen, and F. H. Fu, "A systematic review of the femoral origin and tibial insertion morphology of the acl," *Knee Surgery, Sports Traumatology, Arthroscopy*, vol. 17, no. 3, pp. 213–219, 2009.

[83] R. F. LaPrade, A. H. Engebretsen, T. V. Ly, S. Johansen, F. A. Wentorf, and L. Engebretsen, "The anatomy of the medial part of the knee," *J Bone Joint Surg Am*, vol. 89, no. 9, pp. 2000–2010, 2007.

[84] F. Liu, B. Yue, H. R. Gadikota, M. Kozanek, W. Liu, T. J. Gill, H. E. Rubash, and G. Li, "Morphology of the medial collateral ligament of the knee," *Journal of orthopaedic surgery and research*, vol. 5, no. 1, p. 69, 2010.

[85] J. W. Luites, A. B. Wymenga, L. Blankevoort, and J. G. Kooloos, "Description of the attachment geometry of the anteromedial and posterolateral bundles of the acl from arthroscopic perspective for anatomical tunnel placement," *Knee Surgery, Sports Traumatology, Arthroscopy*, vol. 15, no. 12, pp. 1422–1431, 2007.

[86] S. Takeda, G. Tajima, K. Fujino, J. Yan, Y. Kamei, M. Maruyama, S. Kikuchi, and M. Doita, "Morphology of the femoral insertion of the lateral collateral ligament and popliteus tendon," *Knee Surgery, Sports Traumatology, Arthroscopy*, vol. 23, no. 10, pp. 3049–3054, 2015.

[87] A. Kiapour, A. M. Kiapour, V. Kaul, C. E. Quatman, S. C. Wordeman, T. E. Hewett, C. K. Demetropoulos, and V. K. Goel, "Finite element model of the knee for investigation of injury mechanisms: development and validation," *Journal of biomechanical engineering*, vol. 136, no. 1, p. 011002, 2014.

[88] N. S. Landínez-Parra, D. A. Garzón-Alvarado, and J. C. Vanegas-Acosta, *Mechanical behavior of articular cartilage*. INTECH Open Access Publisher, 2012.

[89] D. Shepherd and B. Seedhom, "Thickness of human articular cartilage in joints of the lower limb," *Annals of the rheumatic diseases*, vol. 58, no. 1, pp. 27–34, 1999.

[90] K. N. Hauch, D. F. Villegas, and T. L. H. Donahue, "Geometry, time-dependent and failure properties of human meniscal attachments," *Journal of biomechanics*, vol. 43, no. 3, pp. 463–468, 2010.

[91] P. Braz and W. Silva, "Meniscus morphometric study in humans," *J Morphol Sci*, vol. 27, no. 2, pp. 62–6, 2010.

[92] N. Rao, A. D. Gupta, and A. Raju, "Morphometric analysis of the menisci of the knee joint in population of east godavari region of andhra pradesh," *Journal of Evolution of Medical and Dental Sciences*, vol. 1, no. 3, pp. 8972–8979.

[93] E. R. Leatherman, H. Guo, S. L. Gilbert, I. D. Hutchinson, S. A. Maher, and T. J. Santner, "Using a statistically calibrated biphasic finite element model of the human knee joint to identify robust designs for a meniscal substitute," *Journal of biomechanical engineering*, vol. 136, no. 7, p. 071007, 2014.

[94] M. A. Baldwin, C. W. Clary, C. K. Fitzpatrick, J. S. Deacy, L. P. Maletsky, and P. J. Rullkoetter, "Dynamic finite element knee simulation for evaluation of knee replacement mechanics," *Journal of Biomechanics*, vol. 45, no. 3, pp. 474–483, 2012.

[95] T. L. H. Donahue, M. Hull, M. M. Rashid, and C. R. Jacobs, "A finite element model of the human knee joint for the study of tibio-femoral contact," *Journal of biomechanical engineering*, vol. 124, no. 3, pp. 273–280, 2002.

[96] K. Quapp and J. Weiss, "Material characterization of human medial collateral ligament," *Journal of biomechanical engineering*, vol. 120, no. 6, pp. 757–763, 1998.

[97] W. Mesfar and A. Shirazi-Adl, "Biomechanics of the knee joint in flexion under various quadriceps forces," *The knee*, vol. 12, no. 6, pp. 424–434, 2005.

[98] Y. Wang, Y. Fan, and M. Zhang, "Comparison of stress on knee cartilage during kneeling and standing using finite element models," *Medical engineering & physics*, vol. 36, no. 4, pp. 439–447, 2014.

[99] M. A. Baldwin, C. Clary, L. P. Maletsky, and P. J. Rullkoetter, "Verification of predicted specimen-specific natural and implanted patellofemoral kinematics during simulated deep knee bend," *Journal of biomechanics*, vol. 42, no. 14, pp. 2341–2348, 2009.

# FINITE ELEMENT ANALYSIS OF CERVICAL SPINE & FINITE ELEMENT MODELING OF KNEE JOINT

ORIGINALITY REPORT

| 14% | 8% | 11% | 2% |
|---|---|---|---|
| SIMILARITY INDEX | INTERNET SOURCES | PUBLICATIONS | STUDENT PAPERS |

PRIMARY SOURCES

| | | |
|---|---|---|
| 1 | Erbulut, D.U., I. Zafarparandeh, I. Lazoglu, and A.F. Ozer. "Application of an asymmetric finite element model of the C2-T1 cervical spine for evaluating the role of soft tissues in stability", Medical Engineering & Physics, 2014.<br>Publication | 1% |
| 2 | Submitted to Bilkent University<br>Student Paper | 1% |
| 3 | etd.lib.metu.edu.tr<br>Internet Source | 1% |
| 4 | Frank Kandziora. "Biomechanical comparison of expandable cages for vertebral body replacement in the cervical spine", Journal of Neurosurgery Spine, 07/2003<br>Publication | <1% |
| 5 | Wollinsky, Jean-Paul, and Reza Yassari. "Atlantoaxial Instability and Stabilization", Schmidek and Sweet s Operative Neurosurgical Techniques, 2012. | <1% |